Identification of Wnt-regulated genes that are repressed by, or independent of, β-catenin

Shiyang Liu[1,2]
Sara Haghani[4]
Enrico Petretto[2, 3]
Babita Madan[1]
Nathan Harmston[1, 4, 5]
David M Virshup[1, 6]

1. Program in Cancer and Stem Cell Biology,
2. Centre for Computational Biology,
3. Program in Cardiovascular and Metabolic Disorders,

All at Duke-NUS School of Medicine, Singapore, 169857

4. Yale-NUS College, Singapore, 138614
5. Cardiff School of Biosciences, Cardiff University, Cardiff, CF10 3AX, UK
6. Department of Pediatrics, Duke University School of Medicine, Durham NC, USA 27710

Address correspondence to Babita Madan, Nathan Harmston and David M Virshup.

Corresponding Authors contact details:
BM, Babita.Madan@duke-nus.edu.sg
NH, HarmstonN@cardiff.ac.uk
DMV, david.virshup@duke.edu

Running title: β-catenin independent and Wnt-repressed genes

Abbreviations: NRE, negative regulatory element; WRE, Wnt-responsive element; TCF, T-cell factor; LEF, Lymphoid Enhancer-binding Factor; TFBS, transcription factor binding site; FDR, False Discovery Rate)

Keywords: Wnt signaling/transcriptional regulation/repression/β-catenin/pancreatic cancer/PORCN

Conflict of interest: Drs. Madan and Virshup have a financial interest in ETC-159.

Abstract

Wnt signaling regulates metazoan development and homeostasis, in part by β-catenin dependent activation and repression of a large number of genes. However, Wnt signaling also regulates genes independent of β-catenin, genes that are less well characterized. In this study, using a pan-Wnt inhibitor, we performed a comprehensive transcriptome analysis in a Wnt-addicted orthotopic cancer model to delineate the β-catenin-dependent and independent arms of Wnt signaling. We find that while a large percentage of Wnt-regulated genes are regulated by β-catenin, 10% of these genes are regulated independent of β-catenin. Interestingly, a large proportion of these β-catenin independent genes are Wnt-repressed. Among the β-catenin dependent genes, more than half are repressed by β-catenin. We used this dataset to investigate the mechanisms by which Wnt/β-catenin signaling represses gene expression, revealing the role of a cis-regulatory motif, the negative regulatory element (NRE). The NRE motif is enriched in the promoters of β-catenin repressed genes and is required for their repression. This provides a comprehensive analysis of the β-catenin independent arm of the Wnt signaling pathway in a cancer model and suggests that a cis-regulatory grammar may determine Wnt-dependent gene activation versus repression.

Introduction

Wnt signaling is an evolutionarily conserved pathway involved in diverse processes including development, homeostasis and tissue regeneration [1]. Dysregulation of this pathway is implicated in myriad diseases including cancer, cardiometabolic disorders and neurodegeneration [2,3]. Signaling is initiated by the binding of Wnt ligands to Frizzleds and other integral membrane co-receptors, which subsequently leads to the activation of distinct downstream signaling pathways. These pathways can operate either through, or independently of, β-catenin, and can either activate or repress specific target genes [4–7].

In the β-catenin-dependent pathway, also known as the canonical pathway, the binding of Wnt ligands to their cognate Frizzled receptors results in the stabilization of β-catenin. This stabilized β-catenin translocates into the nucleus and binds to members of the TCF/LEF family of transcription factors to regulate Wnt-target gene expression in a context-dependent manner [2,8]. In this pathway, the β-catenin/TCF complex binds to DNA through the TCF binding motif, also known as the Wnt-responsive element (WRE) [9]. The β-catenin independent signaling pathways, also known as non-canonical signaling, includes the Wnt/Calcium, Wnt/JNK, Wnt/STOP and planar cell polarity signaling, many of which involve non-canonical Wnts (e.g., WNT5A) and alternative receptors such as ROR. These non-canonical pathways have been implicated in several key cellular processes including migration, planar cell polarity and adhesion that are essential for development and tumorigenesis [10,11]. In contrast to canonical Wnt signaling, our knowledge of the signaling mechanisms and potential target genes in the β-catenin independent arm of the Wnt signaling pathway is less well developed.

The high frequency of mutations leading to aberrant Wnt signaling in multiple tumor types and the changes in transcriptional and cellular states driven by these mutations [12–15] has led to the development of pharmacological approaches to inhibit the pathway [16–18]. One approach is to target Wnt secretion. The post-translational addition of a palmitoleate group to Wnt proteins is necessary for the secretion of all Wnts and is also required for binding to their cognate Frizzled receptor [19–21]. This palmitoleation is catalyzed by the acyltransferase Porcupine (PORCN)[22]. Treatment with small molecule inhibitors of PORCN such as ETC-159 and LGK-974 prevents Wnt palmitoleation and the subsequent inhibition of both the β-catenin-dependent and independent branches of Wnt signaling [23].

Wnt signaling is generally thought of as a pathway for driving the expression of genes, with most of the well characterized Wnt target genes being Wnt-activated, e.g. *AXIN2, MYC* and *Cyclin D1* [24–26]. In contrast, only a limited number of genes repressed by Wnt signaling have been well characterized, *e.g. Mmp7* in mice [27] and *dpp*, *tig*, d*ugt36Bc* in *Drosophila* [28–30] and *BGLAP*, *CDH1* and *CDKN2A* [31,32] in mammalian cells. In our studies investigating the transcriptional response to a pan-Wnt inhibitor in multiple models of Wnt-driven pancreatic and colorectal cancers [7,18], we found that Wnt signaling induces the expression of many genes, *i.e. Wnt-activated*, but that a comparable number of genes were upregulated following Wnt inhibition, hence they were *Wnt-repressed*. Further investigation identified that a subset of these *Wnt-repressed* genes were dependent on the inhibition of MAPK signaling by Wnt/β-catenin signaling [6,33]. However, the mechanisms and

transcriptional elements involved in Wnt signalling-mediated gene repression and the role of β-catenin in this repression is not well understood.

In this study, we performed a comprehensive transcriptome analysis to delineate the β-catenin dependent and independent arms of Wnt signaling. We used a sensitive orthotopic xenograft model of Wnt-driven pancreatic cancer and compared the transcriptional response to a Wnt-secretion inhibitor, ETC-159 in pancreatic tumors without or with ectopically expressed stabilized β-catenin. This analysis revealed that ~90% of Wnt-dependent genes are regulated by β-catenin, while only ~10% are regulated independently of β-catenin. The same dataset was interrogated to better understand how Wnt/β-catenin signaling can repress gene expression. This analysis identified an enrichment of a specific negative regulatory element (NRE) in the promoters of the β-catenin-dependent Wnt-repressed [34]. Our data supports the role of the NRE as an important cis-regulatory motif required for the regulation of β-catenin dependent genes in human cells. This suggests the existence of a cis-regulatory grammar which may be responsible for determining whether a target gene will be repressed or activated by Wnt signaling.

Results

Identification of β-catenin-dependent and -independent Wnt target genes.

HPAF-II cells have an inactivating mutation in RNF43 that drives high autocrine Wnt signaling, making them Wnt-addicted and sensitive to treatment with PORCN inhibitors such as ETC-159 [18,35]. In this context, PORCN inhibition leads to the ablation of both β-catenin dependent and independent Wnt signaling. To dissect the differences between these two branches of the Wnt signaling pathway, we generated HPAF-II cells with constitutively active β-catenin dependent signaling. This was accomplished by stably transducing HPAF-II cells with a plasmid expressing β-catenin with four phosphorylation sites (S33, S37, T41, S45) mutated to alanine, referred to here as β-cat4A [36]. Phosphorylation at these sites by CK1α and GSK3 is required to target β-catenin for proteasomal degradation. As such, treatment of β-cat4A cells with ETC-159 will only affect the expression of Wnt-dependent but β-catenin independent target genes, while genes under the control of β-catenin will be unaffected (**Figure S1A**).

Clones stably expressing β-cat4A were established by single-cell cloning and clones with near-physiological expression levels were selected (**Figure 1A**). To assess the ligand-independent activation of Wnt/β-catenin signaling in these cells we measured their sensitivity to the pan-Wnt inhibitor ETC-159. Confirming the feasibility of this approach, in parental HPAF-II cells (denoted WT in this and subsequent figures), ETC-159 treatment led to a dose-dependent decrease in the expression of the well-characterized Wnt/β-catenin target gene *AXIN2*, while in β-cat4A cells *AXIN2* expression increased at baseline and was not downregulated by Wnt inhibition (**Figure 1B**). Moreover, in a soft agar assay there was only a slight decrease in the β-cat4A colonies even in the presence of 100 nM (~30x the IC50) ETC-

159 (**Figure 1C, S1B**). This demonstrates that the growth of β-cat4A cells in vitro does not require Wnts to activate β-catenin signaling.

To identify β-catenin dependent and independent genes in a more physiological setting, we used an orthotopic xenograft model, where the transcriptional response to Wnt inhibition is significantly more robust than it is *in vitro* or in flank xenografts [7]. WT and β-cat4A HPAF-II cells were injected into the mouse pancreas. Following tumor establishment pan-Wnt inhibition was achieved with ETC-159 (37.5 mg/kg b.i.d. orally) treatment (**Figure 1D**). Gene expression changes were assessed at 4, 16, and 56 h of treatment by RNA-seq. Based on principal component analysis (PCA), the samples clustered as expected (**Figure S1C**). Genes were classified as β-catenin dependent or independent based on their transcriptional response to PORCN inhibition in the presence or absence of stabilized β-catenin (**Table S1**). β-catenin dependent genes were defined as those that were differentially expressed over time in the WT condition (false discovery rate (FDR)<0.1) and responded differently in WT versus β-cat4A tumors (interaction test, FDR<0.1). These criteria resulted in 2988 genes being classified as transcriptional targets of β-catenin dependent signaling. β-catenin independent genes, likely regulated by Wnt-dependent non-canonical pathways, were those that were differentially expressed over time after Wnt inhibition in both β-catenin WT (FDR<0.1) and β-cat4A (FDR<0.1) conditions and whose response to ETC-159 treatment did not significantly differ between conditions (interaction test, FDR>0.1). Using these criteria, 358 genes (~10% of the total number of Wnt-regulated genes) were classified as β-catenin-independent.

To better understand the changes in gene expression, these two sets of genes were clustered based on their temporal response to Wnt inhibition. This identified seven clusters of β-catenin-dependent genes, and three clusters of β-catenin independent genes (**Figure 1E**). DA1-4 (DA = **D**ependent & **A**ctivated) were classified as β-catenin dependent and Wnt-activated, as their expression decreased in response to ETC-159, while DR1-2 (DA = **D**ependent & **R**epressed) were classified as β-catenin dependent and Wnt-repressed, as their expression increased in response to ETC-159 treatment. DN1 (**D**ependent **N**oise) consisted of only nine genes, likely due to clustering artefact. DA1 and DA3 contain most of the well-known direct Wnt-target genes (e.g. *AXIN2, NOTUM, RNF43, MYC, NKD1, BMP4*).

As a proof of concept, we examined *AXIN2*, a well-known direct Wnt-regulated β-catenin target gene. As expected, our analysis classified *AXIN2* as a β-catenin dependent Wnt-activated gene (DA1). In orthotopic HPAF-II tumors, inhibition of Wnt/β-catenin signaling by ETC-159 led to a dramatic downregulation of *AXIN2* expression (FDR=2.58×10^{-132}) (**Figure 2A).** However, in the presence of mutant β-catenin, baseline *AXIN2* expression increased, and Wnt inhibition had no further effect (FDR=0.49). When comparing the expression changes following Wnt inhibition, a significant interaction was observed (interaction test, FDR=196×10^{-58}), indicating a differential response to Wnt inhibition over time depending on the status of β-catenin. Conversely, *DEPTOR* was identified as a β-catenin dependent, Wnt-repressed gene (DR1). It was significantly upregulated in WT tumors following Wnt inhibition (FDR=7.68×10^{-11}) but did not respond to ETC-159 treatment in the presence of mutant β-catenin (FDR=0.52), and these responses were significantly different between the two conditions (interaction test, FDR=0.06) (**Figure 2B**).

Three clusters were identified in the 358 β-catenin independent genes. Cluster IA1 (**I**ndependent & **A**ctivated) was Wnt-activated, while both IR1 and IR2 were Wnt-repressed. *PROCA1* (IA1) and *ABCA6* (IR1) are examples of β-catenin independent genes (**Figures 2C and 2D**) that responded to PORCN inhibition in both the WT and β-cat4A tumors with no significant difference in their response, regardless of the β-catenin protein abundance. Genes in these clusters are presumably regulated by non-canonical Wnt signaling pathways, either directly or indirectly.

We compared the clusters of β-catenin dependent and independent genes with the clusters of Wnt-activated and Wnt-repressed genes identified in [7] (Figure S2) and found them to be largely concordant. This demonstrates reproducibility between independent experiments, supporting the biological relevance of the gene expression patterns we observed.

As an independent validation that our approach identified *bona fide* β-catenin independent targets, we treated the β-cat4A and WT cells with a tankyrase inhibitor, G007LK. G007LK treatment alters β-catenin abundance, impacting the expression of β-catenin target genes without affecting β-catenin independent targets [37]. Similar to the effect of the PORCN inhibitor, G007LK treatment reduced *AXIN2* expression (**Figure S1D)**, but did not reduce the expression of the β-catenin independent genes *KRT19* and *DUSP5* (**Figure S1E-F)**.

HPAF-II tumors are dependent on continuous Wnt signaling, so it was of interest to determine if a further increase in β-catenin caused by ectopic expression of β-cat4A would further change gene expression, or if β-catenin was near-saturating in this system. Of the 2988 β-catenin-dependent Wnt-regulated genes in the HPAF-II orthotopic tumors, only ~10% (296) had significantly higher expression in the tumors with stabilized β-catenin, while 8.6% (258) had a significantly lower expression compared to the WT tumors (**Figure 1E**, column 1). Significant differences were defined as absolute fold-change > 1.5, FDR < 0.1 from their baseline expression, *i.e.* between β-cat4A and WT (**Figure 1F**). As expected, no genes identified as β-catenin-independent were differentially expressed at baseline. This data suggests that this Wnt-addicted cancer has reached close to maximal β-catenin activation.

In summary, transcriptional profiling of our orthotopic *in vivo* model identified a robust set of β-catenin-dependent and -independent target genes, with the β-catenin independent, non-canonical genes accounting for only 10% of the differentially expressed genes in this model. This great difference between the number of β-catenin dependent and β-catenin independent genes indicates that, as least in this context, WNT signaling regulates gene expression predominantly through β-catenin, and/or that non-canonical Wnt signaling may predominantly be acting via non-transcriptional mechanisms.

β-catenin-dependent and -independent Wnt target genes associate with distinct biological pathways.

Functional enrichment analysis was performed to characterize the clusters of β-catenin dependent and independent genes (**Figure 3A, Table S2**). The clusters of Wnt-activated β-catenin dependent genes (DA1-4) were enriched for processes and pathways including Wnt signaling, ribosome biogenesis, DNA replication, splicing and DNA repair, while the Wnt-repressed β-catenin dependent genes (DR1-2) were enriched for protein transport and EGF

signaling pathways. This corroborates an extensive literature on Wnt target genes and our previous findings dissecting the effects of inhibiting the Wnt signaling pathway in RNF43 mutant pancreatic cancer [6,7,33,38,39] and confirms that these processes are regulated downstream of β-catenin.

In contrast, the clusters of β-catenin independent Wnt-activated genes in IA1 showed no significant pathway enrichment. However, genes in the IR2 cluster showed enrichment for processes related to endoderm development, protein O-linked glycosylation and axon guidance, and those in IR1 were enriched for actin organization and cell junction assembly. Taken together, this indicates that the β-catenin dependent and independent branches of the Wnt signaling pathways regulate largely distinct downstream signaling pathways and processes, with non-canonical signaling affecting processes related to development and tissue organization.

β-catenin dependent and independent genes are enriched for distinct transcription factor binding sites.

To identify the transcription factors potentially involved in regulating each of the β-catenin dependent and independent clusters we performed Transcription Factor Binding Site (TFBS) enrichment analysis (**Table S2**) on their promoters, examining sequences 2 kb upstream and 500 bp downstream from their respective transcriptional start site (TSS) (Figure 3B).

β-catenin most famously regulates gene expression by binding to and de-repressing members of the LEF/TCF family of transcription factors, thus activating transcription. Consistent with this, DA1, the cluster containing most of the well-known β-catenin dependent genes showed significant enrichment for TCF7L1 motif, also known as the Wnt-response element, or WRE. DA3 and DA4, clusters enriched for cell cycle related genes (Figure 3A) were also enriched for binding sites for E2F1 and MYC and other key mediators of cell proliferation and mitosis. We note that many relevant LEF/TCF binding sites may be present in enhancers rather than promoters, explaining why they are not strongly enriched in all β-catenin dependent Wnt activated gene clusters. On the other hand, β-catenin-dependent repressed clusters were significantly enriched for binding sites for USF1, JUND and FOXO1.

The β-catenin-independent genes were enriched for a distinct set of TFBSs, with the activated genes showing significant enrichment for RORB binding sites. The β-catenin independent repressed genes were notably enriched for motifs bound by homeobox factors including GSC2, POU6F2, and MSGN1. This finding aligns with the known role of non-canonical Wnt signaling in embryonic development. Overall, the set of enriched motifs were distinct for the dependent and independent genes, consistent with our current understanding that they are regulated by distinct signaling pathways.

A Negative regulatory element (NRE) is enriched in Wnt-dependent gene clusters

An 11-bp sequence, known as the Negative Regulatory Element (NRE) (**Figure 3C**), was previously identified as a motif that modulates the expression of Wnt/β-catenin target genes in *Xenopus laevis*, and was also shown to be functional in mouse embryonic stem cells [34]. This sequence was shown to recruit both TCF and β-catenin, with the binding of both proteins being necessary to mediate its repressive effects. We investigated whether any of the identified

clusters of Wnt-regulated genes were enriched for this motif (**Figure 3C**, Methods). Indeed, we observed an enrichment for a variant of the published NRE element in the Wnt/β-catenin dependent repressed gene clusters with significant enrichment in DR1, suggesting that this motif might be responsible for mediating the expression of a subset of Wnt-repressed target genes.

The NRE motif is enriched in TCF4 and β-catenin ChIP-seq bound peaks

Given the enrichment for the NRE motif in Wnt/β-catenin-repressed genes, we examined publicly available β-catenin and TCF4 (the protein product of the *TCF7L2* gene) ChIP-seq datasets to identify whether the NRE motif was present in regions bound by either of these proteins [40,41]. Analysis of the TCF4 ChIP-seq data obtained from six cell lines found that both the WRE motif and NRE motif were significantly enriched in the TCF4 peaks in all cell lines (**Figure 4A,** Bonferroni corrected p-value < 0.05). The NRE was also significantly enriched compared to random background sequences in the other seven cell-lines, although the enrichment was consistently lower compared to the enrichment observed for the TCF4-binding WRE (**Figure 4A and B**). Analysis of publicly available β-catenin ChIP-seq data generated from DLD1 and SW480 cells also revealed that β-catenin peaks were significantly enriched for both NREs and WREs. In five of the eight cell lines investigated, these two motifs were found to significantly co-occur within peaks more than expected by chance (Fisher's exact test, Bonferroni corrected p-value < 0.05) (**Figure 4C**); however, no preferred distance between NREs and WREs relative to each other was observed (**Figure S3A**). In addition, using publicly available datasets [42,43] we investigated the chromatin binding profiles for components of the LEF/TCF nuclear complex in HEK293T and HEPG2 cells and found significant enrichment for the NRE motif (**Figure S3B-C**). This supports the proposed role of WREs and NREs functioning together to regulate the expression of a target genes in response to Wnt signaling [34].

The negative regulatory element is sufficient to mediate Wnt signaling induced transcriptional repression in human cells.

To functionally assess the role of the NRE in repressing genes in a β-catenin-dependent manner we created three synthetic reporters: i) a minimal reporter (MimRep) that does not respond to Wnt signaling (**Figure S3D**), ii) a 2NRE-reporter containing two 11 bp NRE sites, and iii) a 2WRE-reporter with two WRE sites placed in front of the minimal reporter. In human colorectal cancer HCT116 cells that have hyperactivated Wnt signaling due to a S45del mutation in β-catenin, as expected the 2WRE-reporter showed significantly increased activity, while the 2NRE-reporter activity was repressed compared to the minimal reporter (**Figure 4D**). In contrast, in human fibrosarcoma HT1080 cells with low basal Wnt activity, both the 2NRE-reporter and minimal reporter had similar transcriptional activities, while the 2WRE-reporter showed reduced transcriptional activity (**Figure 4E**). This reduction could potentially be due to the interaction between TCF/LEF and Groucho in the "Wnt-off" condition, which is shown to mediate transcriptional repression of the Wnt activated genes via the WRE [44,45]. These findings suggest that the NRE motif is sufficient to repress reporter activity in a β-catenin-dependent manner in human cancer cell lines.

NREs are necessary for the repression of the Wnt-repressed/β-catenin-dependent lncRNA *ABHD11-AS1*.

As the NRE motif was found to functionally repress reporter activity in HCT116 cells and was enriched in multiple TCF4/β-catenin ChIP-seq datasets, we hypothesized that it may play an important role in regulating a subset of Wnt-repressed/β-catenin-dependent genes in human cancer cells. We previously identified *ABHD11-AS1* as a Wnt-repressed long non-coding RNA (lncRNA) in an orthotopic model of Wnt-addicted pancreatic adenocarcinoma (**Figure 5A**). CRISPRi mediated knockdown of *ABHD11-AS1* led to an increase in the growth of HPAF-II derived subcutaneous tumors, supporting its role as a tumor suppressor *in vivo* (Liu et al., 2020). To test if *ABHD11-AS1* expression is β-catenin-dependent, we treated HT1080 cells with the GSK3 inhibitor BIO that regulates canonical Wnt signaling by stabilizing β-catenin [46]. Treatment of HT1080 cells with BIO led to a significant decrease in *ABHD11-AS1* expression (**Figure 5C**). In both HPAF-II and HCT116 cells that have hyperactivated Wnt signaling due to mutations in *RNF43* and *CTNNB1* respectively, knocking down *CTNNB1* using either CRISPRi in HPAF-II cells (**Figure 5D**), or siRNA in HCT116 cells (**Figure 5E**) led to an increase in *ABHD11-AS1* expression. Furthermore, ETC-159 treatment of HPAF-II cells, inhibiting Wnt secretion, increased *ABHD11-AS1* expression, but this effect was blocked in the presence of stabilized β-catenin (**Figure 5F**). Taken together, these results indicate that *ABHD11-AS1* lncRNA is repressed by β-catenin across multiple cancer cell lines.

We then examined the *ABHD11-AS1* for NREs and WREs. Analysis of the promoter region of *ABHD11-AS1* (3.4 kb upstream and 200 bp downstream of its TSS to the 1st intron) identified two candidate NREs ($P < 2x10^{-4}$), located at 2797 and 1057 bp upstream of the TSS (denoted N1 and N2 respectively), and three candidate WREs ($P < 6x10^{-4}$), located 2785, 1462 and 1075 bp upstream of the TSS (**Figure 5B**). To elucidate the role of NREs in the regulation of *ABHD11-AS1*, we cloned its promoter region, from 3327 bp upstream to 151 bp downstream of its TSS, into a luciferase reporter pGL4.20. We then systematically deleted regions of the promoter to remove NREs and measured the resulting reporter activity in HCT116 cells. Deleting a region containing N1 (ΔN1, W1), led to a 1.6-fold increase in reporter activity compared to the full length (FL) construct (**Figure 5G**), suggesting that NRE (N1) represses *ABHD11-AS1* expression. Further deletion of a 1265 bp fragment (ΔW2), with no identifiable NREs, did not change the transcriptional activity (**Figure 5G**). However, deleting a 400 bp DNA fragment containing N2 (ΔN2, W3), led to a 2.9-fold increase in the reporter activity (**Figure 5G**). This suggests that NREs are required for repressing the expression of *ABHD11-AS1*.

Large deletions of the promoter fragment could potentially lead to the loss of additional functional elements besides the NREs. Therefore, to specifically investigate the effect of NREs on the *ABHD11-AS1* regulation, we performed a series of mutagenesis experiments (**Figure 5H**). It has been shown that mutating the 11th base of the NRE motif can reduce its suppressive function [34]. We therefore mutated the last base of each of the two NREs (Mut N1, Mut N2) in the 3478-bp promoter fragment. Each of these mutants significantly enhanced reporter activity to a level comparable to that observed following deletion of N1 (ΔN1) harboring regions. However, the reporter activity of the N2 mutant was further increased by deletion of both the NRE and WRE elements (**Figure 5H**, compare ΔW2 Mut N2 with ΔN2, W3),

suggesting that a single bp change does not completely abrogate the NRE function, and/or that the interaction with the WRE element is required for the repression. Taken together, these data show that perturbation of NREs in the *ABHD11-AS1* promoter leads to its activation, confirming that NREs are functional motifs that are capable of repressing gene expression in a Wnt-dependent manner in human cancer cells.

NRE modulates the expression of Wnt-activated/β-catenin-dependent gene *AXIN2*.

Kim *et al.* suggested that β-catenin binds to both NREs as well as WREs to modulate the expression of the Wnt-activated genes *siamois* in *Xenopus* and *Brachyury* in mESCs [34]. To test the hypothesis that NREs can modulate Wnt-activated/β-catenin-dependent genes, we examined *AXIN2,* a well-established β-catenin dependent Wnt-activated gene (**Figure 6A**). Scanning the human *AXIN2* promoter region (from 3.5 kb upstream to 1 kb downstream of its TSS), we identified seven WREs ($P < 1.5x10^{-4}$) (**Figure 6B**) with five located within the first intron and two within the 1 kb of its TSS. In addition, we also identified one NRE (P < 1.5e-04) located 1329 bp upstream from the TSS (**Figure 6B**).

We confirmed that *AXIN2* is a Wnt-activated/β-catenin-dependent gene in various *in vitro* models (**Figure S4A-C**). As expected, *AXIN2* was upregulated following BIO treatment in HT1080 cells and was downregulated by using either CRISPRi or siRNA knockdown of β-catenin in HPAF-II and HCT116 cells. In addition, *AXIN2* was significantly upregulated in β-cat4A HPAF-II and did not respond to PORCN inhibition unlike the HPAF-II WT cells (**Figure S4D**).

To study the functional importance of NREs in the regulation of *AXIN2* expression, we cloned the *AXIN2* promoter region from 2012 bp upstream to 1261 bp downstream of its TSS into a luciferase reporter. Removing the DNA region containing N1 (ΔN1) in this 3273 bp promoter fragment increased the reporter activity by 3-fold in HCT116 cells (**Figure 6C**). Similarly, mutating multiple nucleotides in the poly(thymine) region of NRE N1 to guanine (Mut N1), also significantly enhanced the reporter activity by 2.1-fold (**Figure 6D**). As expected, removing the DNA sequence containing WREs led to a significant decrease in reporter activity (**Figure 6C**). Thus, the NRE can modulate expression of both Wnt/β-catenin repressed and Wnt /β-catenin-activated target genes.

Discussion

Wnt signaling is a potent regulator of gene expression, which is achieved primarily via changes in nuclear β-catenin abundance. In addition, diverse β-catenin-independent Wnt-regulated (non-canonical) pathways have also been described. However, the contribution of these pathways to the Wnt-regulated transcriptional response is poorly understood. Here, using a PORCN inhibitor that blocks the secretion of all Wnts in a robust orthotopic xenograft cancer model, we find that the majority of Wnt-regulated genes (~90%) are regulated by changes in β-catenin abundance, indicating that the Wnt-regulated non-canonical pathways, at least in this cancer model, have a small transcriptional impact. Furthermore, this dataset was also interrogated to better understand how Wnt/β-catenin signaling can repress gene expression. This analysis confirms and refines the role of a specific negative Regulatory Element (NRE),

extending our understanding of a how β-catenin can repress and/or modulate Wnt-regulated genes.

β-catenin independent roles of Wnt signaling have been well-described. Non-canonical Wnt signaling calcium transients can activate PKC and/or CAMKII, while planar cell polarity signaling functions in part via monomeric GTPase and activation of JNK [47,48]. The consequence of regulating these pathways is cytoskeletal or synaptic reorganization [49,50]. While Wnt-JNK signaling can activate gene expression in Xenopus there is little evidence this pathway regulates transcription in mammals [51] . Finally, Wnt/STOP signaling increases the proteolysis of proteins including transcription factors such as MYC [5,7,52] but how much they alter gene expression in a physiologic setting is not known. While we cannot separate out the contribution of each of these preceding pathways, our data suggests that taken together, the contribution of these pathways to transcriptional regulation is limited to only 10% of the Wnt-regulated genes. These β-catenin independent genes were enriched for developmental pathways and consistent with that, they showed an enrichment for the transcription factor binding sites for homeobox factors including GSC2, POU6F2 and MSGN1.

There are three strengths of our experimental system. First, we used a cancer model driven by an RNF43 mutation that sensitizes tumor cells to all Wnts, both canonical and non-canonical. Second, using an orthotopic xenograft mode provides a more physiologic milieu, making it far more robust in identifying Wnt-regulated genes than either non-orthotopic xenografts (usually flank) or tissue culture models [7]. Finally, using a drug that rapidly inactivates Wnt secretion and harvesting the tumors at early time points maximizes the identification of direct targets of the Wnt pathway. This approach provided clear insights into the Wnt-regulated transcriptome.

One striking finding in this and our prior studies is that although there are similar number of genes that are repressed versus activated by Wnt signaling, only a limited number Wnt repressed genes have been identified previously. Here we show that most of these Wnt-repressed genes are still regulated by β-catenin. Several mechanisms have been proposed to explain direct β-catenin/TCF dependent gene repression. This repression was shown to be mediated by binding of TCFs to Wnt Response Elements (WREs). For example, the positioning of WREs in relation to the transcription start site of *MMP7* was shown to be critical for determining its effect on gene expression [27]. In Drosophila, Wnt/β-catenin signaling represses *stripe* expression at the parasegment boundary during development by steric competition between TCF/LEF (Pangolin) and the transcriptional activator Ci at partially overlapping binding sites [53]. In mice during hair follicle bud development Wnt/β-catenin signaling represses E-cadherin [54] by TCF binding to WRE, which then recruits the transcriptional repressor Snail.

Here we confirm and extend the identification of a negative regulatory element (NRE), where β-catenin interacts with transcription factors such as TCF to repress gene expression. This is consistent with prior work that identified non-canonical TCF binding sites involved in gene repression. For example, a non-canonical TCF site repressed *Ugt36Bc* expression in Drosophila [28] and a novel bipartite TCF binding sequence mediating repression was identified in the fly lymph gland [29]. Other studies have suggested that Wnt-mediated

repression works by TCF forming a complex with another TF such as GATA3, forming a repressive complex [41].

Kim et al. identified an 11 bp repressive motif termed the Negative Regulatory Element often present alongside the canonical WRE in Wnt-regulated genes [34] that was shown to interact with both TCF and β-catenin proteins. While TCF can bind to the NRE, β-catenin may also form repressive complexes with transcription factors other than TCF/LEF that could also interact with this element. Our study confirms that the NRE, albeit with a modified sequence, is enriched in a subset of Wnt-repressed genes. Our mutagenesis studies show that the NRE directs β-catenin dependent repression of the long non-coding RNA *ABHD11-AS1*, and interestingly, also modulates the expression of the robustly Wnt-activated gene *AXIN2*. Overall, this study supports the role of the NRE as an important *cis*-regulatory motif regulating Wnt target genes in human cells and suggests a *cis*-regulatory grammar which can determine whether a target gene will be repressed or activated by Wnt signaling.

We observed 10% of Wnt-regulated genes to be β-catenin independent. This may be due to the high sensitivity of a cancer cell line used in this study that may have shaped the Wnt-regulated transcriptome to favor expression of β-catenin dependent genes. It is also possible that the β-catenin independent gene expression may be more common in normal tissue homeostasis and/or developmental stages. These questions can be addressed in future studies.

In conclusion, this study provides a comprehensive analysis of the β-catenin dependent vs independent genes in a cancer model and advances our knowledge of the role of a cis-regulatory motif in regulating the expression of Wnt target genes in human cells.

Materials and Methods

Study approval

NOD SCID gamma mice were purchased from InVivos, Singapore and from Jackson Laboratories, Bar Harbor, Maine. All animal studies were approved by the SingHealth Institutional Animal Care and Use Committee (IACUC # 2014/SHS/975) and adhered to relevant regulations. A total of 32 mice, both male and female, were used for the study and housed in standard cages and had unrestricted access to food and water.

RNA-seq

Briefly, HPAF-II cells obtained from ATCC (RRID:CVCL_0313) with stable expression of firefly luciferase with and without stable expression of mutant β-catenin were orthotopically injected into the pancreas of NSG mice, as previously described. Approximately 4 weeks later, mice were treated with ETC-159 or vehicle as indicated and then sacrificed at the indicated time points. RNAseq was performed on harvested tumors as previously described [7].

Data processing and quality control:

Due to potential stromal contamination arising from the use of an orthotopic mouse model Xenome was used prior to alignment to remove murine (mm10) reads [55] . FastQC was used to ensure the overall quality of the sequences. The remaining reads were then aligned against hg38 (Ensembl version 100) using STAR v2.7.1a [56] and RSEM v1.3.1[57] . Genes which had less than 10 reads mapping on average over all samples, as well as reads mapping to rRNA, mtRNA, snoRNA, and snRNA were filtered out. Differentially expressed genes were identified using DEseq2 [58] . Independent filtering was not used in this analysis.

Identification of β-catenin-dependent and independent clusters:

DESeq2 was used to identify genes that responded differently to ETC-159 treatment depending on CTNNB1 status. Gene expression changes were modelled as y ~ condition + timepoint + condition:timepoint, where condition is wildtype (WT) or mutant (Mut) and timepoint is 0 h, 4 h, 16 h, 56 h. Likelihood ratio tests were also performed to identify genes that changed expression significantly across time within conditions. Pairwise comparison using Wald test was performed between WT and Mut conditions at 0 h to identify genes with differences in baseline expression. Coefficients from the model (representing log fold changes) were clustered using k-means clustering, with the value of k being determined using the elbow criterion.

Functional enrichment analysis:

Gene Ontology (GO) enrichment was performed using enrichGO and pathway enrichments using enrichKEGG from ClusterProfiler [59] using all expressed genes as background. Terms with FDR < 0.1 were defined as being significantly enriched.

Motif enrichment analysis:

Promoters were defined as 2000 bp upstream and 500 bp downstream or as stated in the results. Enrichment analysis was performed using monaLisa [60] using JASPAR2020 [61], min.score 80%, binomial test, all promoters used as background, genome oversample 20.

NRE motif

The NRE motif was derived from the sequences reported [34], however the sequences for Brachyury-1 and Brachyury-2 were reverse complemented before generation of the position frequency matrix. The position frequency matrix was built following the same methods [62] by aligning 11-bp NRE sequences using TFBSTools [63] .

ChIP-seq

CTNNB1 and TCF7L2 ChIP-seq data was downloaded from GEO [40,41]. FastQC was used to perform quality checks on raw sequence data and adapters were trimmed using cutadapt. Reads were aligned against the human genome (hg38) using BWA [64] and peaks were identified using MACS2, using default parameters [65]. ChIPQC was used to assess the quality of ChIP-seq samples and experiments [66]. For samples where replicates were available, an irreproducible discovery rate (IDR) threshold of 0.05 was used to select for highly

reproducible peaks [67]. Peaks were centered on their midpoint and resized to 500 bp for analysis.

Motif enrichment and identification was performed using MEME [68]. SpaMo was used to determine whether there were significantly enriched spacings between the NRE and WRE motifs [69] . Default parameters used with the margin size of 150 bp.

Motif identification

ABHD11-AS1 promoter region (3.4 kb upstream and 200 bp downstream of its TSS) and *AXIN2* promoter region (3.5 kb upstream to 1 kb downstream of its TSS) were used as input using FIMO [70] to scan for putative NRE and WRE sites with default settings and threshold 1e-3. The NRE motif file was generated as described above. The WRE motif was downloaded from JASPAR2020 with ID MA0523.1. We used the associated P value to filter out those less plausible sites in terms of computational prediction and then subjected remaining potential NRE and WRE sites reporter assay to test their functionality.

Construction of ABHD11-AS1 and AXIN2 promoter reporters to assess the effect of NRE truncation and mutation on promoter activity

ABHD11-AS1 promoter region from 3327 bp upstream to 151 bp downstream of its TSS and *AXIN2* promoter region from 2012 bp upstream to 1261 bp downstream of its TSS were cloned from genomic DNA with primer sequences listed in Table S3. The promoter regions were cloned into the luciferase reporter pGL4.20 (Promega) with NheI and HindIII restriction sites (named as FL construct). A series of deletion constructs were generated using FL as a template with primers sequences listed in Table S3. All PCR products were digested with NheI and HindIII and cloned into pGL4.20 (Promega). Site-directed mutagenesis was performed to mutate NRE with primers listed in table S3.

Construction of minimal reporter

311 bp (without any putative NREs or WREs) from the ABHD11-AS1 promoter region (sequences listed in Table S3) was cloned into the pGL4.20 (basic vector with no promoter) with NheI and HindIII restriction sites to construct a MimRep. Two NREs and 2 WREs sequences (listed in Table S3) were cloned into the MimRep with SacI and KpnI restriction sites to construct 2NRE-Reporter and 2WRE-Reporter.

Luciferase assay

HCT116 (RRID:CVCL_0291) or HT1080 (RRID:CVCL_0317) cells were obtained from ATCC and were seeded into 24-well plates one day before transfection. Cells were transfected with different constructs and control Renilla luciferase expression vector using Lipofectamine 2000 (Invitrogen) according to manufacturer's instructions. Luciferase activity was assessed 24 h after transfection with the Dual-Luciferase Reporter Assay System (Promega) as previously described [71] . Transfections were performed at least in triplicate on at least two separate experiments. Luciferase signals were first normalized to Renilla. The relative amount of luciferase activity was further normalized to the empty vector (pGL4.20) transfected cells. All experiments were performed with mycoplasma-free cells.

CRISPRi Knock down studies

The sgRNAs were cloned into doxycycline-inducible lentiviral sgRNA expression vector FgH1tUTG as previously described [72] . The sgRNA plasmid was packaged into lentiviral particles with psPAX2 and pMD2.G packaging plasmids. The virus supernatant was harvested 48 and 72 h after transfection, filtered through 0.45-μm filter, and stored at − 80 °C. For individual sgRNA knockdown using doxycycline-inducible lentiviral sgRNA expression vector FgH1tUTG, 1 μg/ml doxycycline final concentration (dox) (from a stock of 10 mg/ml dissolved in DMSO) was used to induce sgRNA expression from the system, while DMSO was used as the control. After 48 h induction, total RNA was isolated from the CRISPRi knockdown cells. RT-qPCR was performed to assess the knockdown efficiency for *CTNNB1* with *EPN1* gene as an internal control. RT-qPCR primers are listed in Table S3.

Author Contributions

SL, BM, NH, EP and DMV designed the study and planned experiments. SL and BM performed experiments. SL, SH, BM and NH analysed data. All authors were involved in interpretation of the data. SL, BM, NH and DMV wrote the manuscript.

Acknowledgements

This work was supported by National University of Singapore and Yale-NUS College (through Reimagine Research Grant IG20-RRSG-001 to N.H.), STAR Award MOH-000155 to D.M.V. and OFIRG/0055/2017 to Babita Madan from the National Research Foundation Singapore, administered by the Singapore Ministry of Health's National Medical Research Council. The sponsors had no role in the study design, in the collection, analysis and interpretation of data; in the writing of the report; and in the decision to submit the article for publication. Components of the Bioinformatics analysis was performed on the Cardiff School of Biosciences' Biocomputing Hub HPC/Cloud infrastructure (Resources funded by the Cardiff School of Biosciences).

Data availability

RNA-Seq data is available in the NCBI Gene Expression Omnibus (GEO; http://www.ncbi.nlm.nih.gov/geo/) under accession number GSE291732. All analysis code is available at: https://github.com/harmstonlab/wnt_nre_manuscript

References

1 Steinhart Z & Angers S (2018) Wnt signaling in development and tissue homeostasis. *Development* **145**, dev146589.

2 MacDonald BT, Tamai K & He X (2009) Wnt/β-Catenin Signaling: Components, Mechanisms, and Diseases. *Dev Cell* **17**, 9–26.

3 Nusse R & Clevers H (2017) Wnt/β-Catenin Signaling, Disease, and Emerging Therapeutic Modalities. *Cell* **169**, 985–999.

4 Wiese KE, Nusse R & Amerongen R van (2018) Wnt signalling: conquering complexity. *Development* **145**, dev165902.

5 Acebron SP & Niehrs C (2016) β-Catenin-Independent Roles of Wnt/LRP6 Signaling. *Trends Cell Biol* **26**, 956–967.

6 Harmston N, Lim JYS, Arqués O, Palmer HG, Petretto E, Virshup DM & Madan B (2021) Widespread Repression of Gene Expression in Cancer by a Wnt/β-Catenin/MAPK Pathway. *Cancer Res* **81**, 464–475.

7 Madan B, Harmston N, Nallan G, Montoya A, Faull P, Petretto E & Virshup DM (2018) Temporal dynamics of Wnt-dependent transcriptome reveals an oncogenic Wnt/MYC/ribosome axis. *J Clin Investig* **128**, 5620–5633.

8 Nakamura Y, Alves E de P, Veenstra GJC & Hoppler S (2016) Tissue- and stage-specific Wnt target gene expression is controlled subsequent to β-catenin recruitment to cis-regulatory modules. *Dev (Camb, Engl)* **143**, 1914–1925.

9 Wetering M van de, Cavallo R, Dooijes D, Beest M van, Es J van, Loureiro J, Ypma A, Hursh D, Jones T, Bejsovec A, Peifer M, Mortin M & Clevers H (1997) Armadillo coactivates transcription driven by the product of the Drosophila segment polarity gene dTCF. *Cell* **88**, 789–99.

10 Yang Y & Mlodzik M (2015) Wnt-Frizzled/Planar Cell Polarity Signaling: Cellular Orientation by Facing the Wind (Wnt). *Annu Rev Cell Dev Biol* **31**, 623–646.

11 Schlessinger K, Hall A & Tolwinski N (2009) Wnt signaling pathways meet Rho GTPases. *Genes Dev* **23**, 265–277.

12 Aoki K & Taketo MM (2007) Adenomatous polyposis coli (APC): a multi-functional tumor suppressor gene. *J Cell Sci* **120**, 3327–3335.

606 13 Zhong Z, Yu J, Virshup DM & Madan B (2020) Wnts and the hallmarks of cancer. *Cancer Metastasis Rev* **39**, 625–645.

608 14 Seshagiri S, Stawiski EW, Durinck S, Modrusan Z, Storm EE, Conboy CB, Chaudhuri S, Guan Y, Janakiraman V, Jaiswal BS, Guillory J, Ha C, Dijkgraaf GJP, Stinson J, Gnad F, 610 Huntley MA, Degenhardt JD, Haverty PM, Bourgon R, Wang W, Koeppen H, Gentleman R, Starr TK, Zhang Z, Largaespada DA, Wu TD & Sauvage FJ de (2012) Recurrent R- 612 spondin fusions in colon cancer. *Nature* **488**, 660–664.

15 Jiang X, Hao H-X, Growney JD, Woolfenden S, Bottiglio C, Ng N, Lu B, Hsieh MH, 614 Bagdasarian L, Meyer R, Smith TR, Avello M, Charlat O, Xie Y, Porter JA, Pan S, Liu J, McLaughlin ME & Cong F (2013) Inactivating mutations of RNF43 confer Wnt 616 dependency in pancreatic ductal adenocarcinoma. *Proc Natl Acad Sci* **110**, 12649–12654.

16 Huang S-MA, Mishina YM, Liu S, Cheung A, Stegmeier F, Michaud GA, Charlat O, 618 Wiellette E, Zhang Y, Wiessner S, Hild M, Shi X, Wilson CJ, Mickanin C, Myer V, Fazal A, Tomlinson R, Serluca F, Shao W, Cheng H, Shultz M, Rau C, Schirle M, Schlegl J, 620 Ghidelli S, Fawell S, Lu C, Curtis D, Kirschner MW, Lengauer C, Finan PM, Tallarico JA, Bouwmeester T, Porter JA, Bauer A & Cong F (2009) Tankyrase inhibition stabilizes 622 axin and antagonizes Wnt signalling. *Nature* **461**, 614–620.

17 Steinhart Z, Pavlovic Z, Chandrashekhar M, Hart T, Wang X, Zhang X, Robitaille M, 624 Brown KR, Jaksani S, Overmeer R, Boj SF, Adams J, Pan J, Clevers H, Sidhu S, Moffat J & Angers S (2017) Genome-wide CRISPR screens reveal a Wnt–FZD5 signaling circuit 626 as a druggable vulnerability of RNF43-mutant pancreatic tumors. *Nat Med* **23**, 60–68.

18 Madan B, Ke Z, Harmston N, Ho SY, Frois AO, Alam J, Jeyaraj DA, Pendharkar V, 628 Ghosh K, Virshup IH, Manoharan V, Ong EHQ, Sangthongpitag K, Hill J, Petretto E, Keller TH, Lee MA, Matter A & Virshup DM (2016) Wnt addiction of genetically defined 630 cancers reversed by PORCN inhibition. *Oncogene* **35**, 2197–2207.

19 Coombs GS, Yu J, Canning CA, Veltri CA, Covey TM, Cheong JK, Utomo V, Banerjee 632 N, Zhang ZH, Jadulco RC, Concepcion GP, Bugni TS, Harper MK, Mihalek I, Jones CM, Ireland CM & Virshup DM (2010) WLS-dependent secretion of WNT3A requires Ser209 634 acylation and vacuolar acidification. *J Cell Sci* **123**, 3357–3367.

20 Lum L & Clevers H (2012) The Unusual Case of Porcupine. *Science* **337**, 922–923.

636 21 Proffitt KD, Madan B, Ke Z, Pendharkar V, Ding L, Lee MA, Hannoush RN & Virshup DM (2013) Pharmacological Inhibition of the Wnt Acyltransferase PORCN Prevents 638 Growth of WNT-Driven Mammary Cancer. *Cancer Res* **73**, 502–507.

22 Takada R, Satomi Y, Kurata T, Ueno N, Norioka S, Kondoh H, Takao T & Takada S 640 (2006) Monounsaturated Fatty Acid Modification of Wnt Protein: Its Role in Wnt Secretion. *Dev Cell* **11**, 791–801.

642 23 Madan B & Virshup DM (2015) Targeting Wnts at the Source—New Mechanisms, New Biomarkers, New Drugs. *Mol Cancer Ther* **14**, 1087–1094.

644 24 Tetsu O & McCormick F (1999) β-Catenin regulates expression of cyclin D1 in colon carcinoma cells. *Nature* **398**, 422–426.

646 25 Jho E, Zhang T, Domon C, Joo C-K, Freund J-N & Costantini F (2002) Wnt/beta-catenin/Tcf signaling induces the transcription of Axin2, a negative regulator of the
648 signaling pathway. *Molecular and Cellular Biology* **22**, 1172–1183.

26 He T-C, Sparks AB, Rago C, Hermeking H, Zawel L, Costa LT da, Morin PJ, Vogelstein
650 B & Kinzler KW (1998) Identification of c-MYC as a Target of the APC Pathway. *Science* **281**, 1509–1512.

652 27 Gustavson MD, Crawford HC, Fingleton B & Matrisian LM (2004) Tcf binding sequence and position determines β-catenin and Lef-1 responsiveness of MMP-7 promoters. *Mol*
654 *Carcinog* **41**, 125–139.

28 Blauwkamp TA, Chang MV & Cadigan KM (2008) Novel TCF-binding sites specify
656 transcriptional repression by Wnt signalling. *EMBO J* **27**, 1436–1446.

29 Zhang CU, Blauwkamp TA, Burby PE & Cadigan KM (2014) Wnt-Mediated Repression
658 via Bipartite DNA Recognition by TCF in the Drosophila Hematopoietic System. *PLoS Genet* **10**, e1004509.

660 30 Theisen H, Syed A, Nguyen BT, Lukacsovich T, Purcell J, Srivastava GP, Iron D, Gaudenz K, Nie Q, Wan FYM, Waterman ML & Marsh JL (2007) Wingless Directly
662 Represses DPP Morphogen Expression via an Armadillo/TCF/Brinker Complex. *PLoS ONE* **2**, e142.

664 31 Saller E, Kelley A & Bienz M (2002) The transcriptional repressor Brinker antagonizes Wingless signaling. *Genes Dev* **16**, 1828–1838.

666 32 Hoverter NP & Waterman ML (2008) A Wnt-fall for gene regulation: repression. *Sci Signal* **1**, pe43–pe43.

668 33 Madan B, Wadia SR, Patnaik S, Harmston N, Tan EKW, Tan IBH, Nes WD, Petretto E & Virshup DM (2024) The cholesterol biosynthesis enzyme FAXDC2 couples Wnt/β-
670 catenin to RTK/MAPK signaling. *J Clin Investig* **134**, e171222.

34 Kim K, Cho J, Hilzinger TS, Nunns H, Liu A, Ryba BE & Goentoro L (2017) Two-
672 Element Transcriptional Regulation in the Canonical Wnt Pathway. *Current Biology* **27**, 2357-2364.e5.

674 35 Liu J, Pan S, Hsieh MH, Ng N, Sun F, Wang T, Kasibhatla S, Schuller AG, Li AG, Cheng D, Li J, Tompkins C, Pferdekamper A, Steffy A, Cheng J, Kowal C, Phung V, Guo G,
676 Wang Y, Graham MP, Flynn S, Brenner JC, Li C, Villarroel MC, Schultz PG, Wu X, McNamara P, Sellers WR, Petruzzelli L, Boral AL, Seidel HM, McLaughlin ME, Che J,
678 Carey TE, Vanasse G & Harris JL (2013) Targeting Wnt-driven cancer through the inhibition of Porcupine by LGK974. *Proc National Acad Sci* **110**, 20224–20229.

680 36 Fuerer C & Nusse R (2010) Lentiviral Vectors to Probe and Manipulate the Wnt Signaling Pathway. *Plos One* **5**, e9370.

682 37 Lau T, Chan E, Callow M, Waaler J, Boggs J, Blake RA, Magnuson S, Sambrone A, Schutten M, Firestein R, Machon O, Korinek V, Choo E, Diaz D, Merchant M, Polakis P,
684 Holsworth DD, Krauss S & Costa M (2013) A novel tankyrase small-molecule inhibitor suppresses APC mutation-driven colorectal tumor growth. *Cancer Research* **73**, 3132–
686 3144.

38 Idris M, Harmston N, Petretto E, Madan B & Virshup DM (2019) Broad regulation of
688 gene isoform expression by Wnt signaling in cancer. *Rna* **25**, 1696–1713.

39 Kaur A, Lim JYS, Sepramaniam S, Patnaik S, Harmston N, Lee MA, Petretto E, Virshup
690 DM & Madan B (2021) WNT inhibition creates a BRCA-like state in Wnt-addicted cancer. *Embo Mol Med* **13**, e13349.

692 40 Wan C, Mahara S, Sun C, Doan A, Chua HK, Xu D, Bian J, Li Y, Zhu D, Sooraj D, Cierpicki T, Grembecka J & Firestein R (2021) Genome-scale CRISPR-Cas9 screen of
694 Wnt/β-catenin signaling identifies therapeutic targets for colorectal cancer. *Sci Adv* **7**, eabf2567.

696 41 Frietze S, Wang R, Yao L, Tak YG, Ye Z, Gaddis M, Witt H, Farnham PJ & Jin VX (2012) Cell type-specific binding patterns reveal that TCF7L2 can be tethered to the
698 genome by association with GATA3. *Genome biology* **13**, R52.

42 Zambanini G, Nordin A, Jonasson M, Pagella P & Cantù C (2022) A new cut&run low
700 volume-urea (LoV-U) protocol optimized for transcriptional co-factors uncovers Wnt/b-catenin tissue-specific genomic targets. *Development* **149**, dev201124.

702 43 Dunham I, Kundaje A, Aldred SF, Collins PJ, Davis CA, Doyle F, Epstein CB, Frietze S, Harrow J, Kaul R, Khatun J, Lajoie BR, Landt SG, Lee B-K, Pauli F, Rosenbloom KR,
704 Sabo P, Safi A, Sanyal A, Shoresh N, Simon JM, Song L, Trinklein ND, Altshuler RC, Birney E, Brown JB, Cheng C, Djebali S, Dong X, Dunham I, Ernst J, Furey TS, Gerstein
706 M, Giardine B, Greven M, Hardison RC, Harris RS, Herrero J, Hoffman MM, Iyer S, Kellis M, Khatun J, Kheradpour P, Kundaje A, Lassmann T, Li Q, Lin X, Marinov GK,
708 Merkel A, Mortazavi A, Parker SCJ, Reddy TE, Rozowsky J, Schlesinger F, Thurman RE, Wang J, Ward LD, Whitfield TW, Wilder SP, Wu W, Xi HS, Yip KY, Zhuang J,
710 Bernstein BE, Birney E, Dunham I, Green ED, Gunter C, Snyder M, Pazin MJ, Lowdon RF, Dillon LAL, Adams LB, Kelly CJ, Zhang J, Wexler JR, Green ED, Good PJ, Feingold
712 EA, Bernstein BE, Birney E, Crawford GE, Dekker J, Elnitski L, Farnham PJ, Gerstein M, Giddings MC, Gingeras TR, Green ED, Guigó R, Hardison RC, Hubbard TJ, Kellis M,
714 Kent WJ, Lieb JD, Margulies EH, Myers RM, Snyder M, Stamatoyannopoulos JA, Tenenbaum SA, Weng Z, White KP, Wold B, Khatun J, Yu Y, Wrobel J, Risk BA,
716 Gunawardena HP, Kuiper HC, Maier CW, Xie L, Chen X, Giddings MC, Bernstein BE, Epstein CB, Shoresh N, Ernst J, Kheradpour P, Mikkelsen TS, Gillespie S, Goren A, Ram
718 O, Zhang X, Wang L, Issner R, Coyne MJ, Durham T, Ku M, Truong T, Ward LD, Altshuler RC, Eaton ML, Kellis M, Djebali S, Davis CA, Merkel A, Dobin A, Lassmann
720 T, Mortazavi A, Tanzer A, Lagarde J, Lin W, Schlesinger F, Xue C, Marinov GK, Khatun J, Williams BA, Zaleski C, Rozowsky J, Röder M, Kokocinski F, Abdelhamid RF, Alioto
722 T, Antoshechkin I, Baer MT, Batut P, Bell I, Bell K, Chakrabortty S, Chen X, Chrast J, Curado J, Derrien T, Drenkow J, Dumais E, Dumais J, Duttagupta R, Fastuca M, Fejes-
724 Toth K, Ferreira P, Foissac S, Fullwood MJ, Gao H, Gonzalez D, Gordon A, Gunawardena HP, Howald C, Jha S, Johnson R, Kapranov P, King B, Kingswood C, Li G,

726 Luo OJ, Park E, Preall JB, Presaud K, Ribeca P, Risk BA, Robyr D, Ruan X, Sammeth M, Sandhu KS, Schaeffer L, See L-H, Shahab A, Skancke J, Suzuki AM, Takahashi H,
728 Tilgner H, Trout D, Walters N, Wang H, Wrobel J, Yu Y, Hayashizaki Y, Harrow J, Gerstein M, Hubbard TJ, Reymond A, Antonarakis SE, Hannon GJ, Giddings MC, Ruan
730 Y, Wold B, Carninci P, Guigó R, Gingeras TR, Rosenbloom KR, Sloan CA, Learned K, Malladi VS, Wong MC, Barber GP, Cline MS, Dreszer TR, Heitner SG, Karolchik D,
732 Kent WJ, Kirkup VM, Meyer LR, Long JC, Maddren M, Raney BJ, Furey TS, Song L, Grasfeder LL, Giresi PG, Lee B-K, Battenhouse A, Sheffield NC, Simon JM, Showers
734 KA, Safi A, London D, Bhinge AA, Shestak C, Schaner MR, Kim SK, Zhang ZZ, Mieczkowski PA, Mieczkowska JO, Liu Z, McDaniell RM, Ni Y, Rashid NU, Kim MJ,
736 Adar S, Zhang Z, Wang T, Winter D, Keefe D, Birney E, Iyer VR, Lieb JD, Crawford GE, Li G, Sandhu KS, Zheng M, Wang P, Luo OJ, Shahab A, Fullwood MJ, Ruan X, Ruan Y,
738 Myers RM, Pauli F, Williams BA, Gertz J, Marinov GK, Reddy TE, Vielmetter J, Partridge E, Trout D, Varley KE, Gasper C, Bansal A, Pepke S, Jain P, Amrhein H,
740 Bowling KM, Anaya M, Cross MK, King B, Muratet MA, Antoshechkin I, Newberry KM, McCue K, Nesmith AS, Fisher-Aylor KI, Pusey B, DeSalvo G, Parker SL,
742 Balasubramanian S, Davis NS, Meadows SK, Eggleston T, Gunter C, Newberry JS, Levy SE, Absher DM, Mortazavi A, Wong WH, Wold B, Blow MJ, Visel A, Pennachio LA,
744 Elnitski L, Margulies EH, Parker SCJ, Petrykowska HM, Abyzov A, Aken B, Barrell D, Barson G, Berry A, Bignell A, Boychenko V, Bussotti G, Chrast J, Davidson C, Derrien
746 T, Despacio-Reyes G, Diekhans M, Ezkurdia I, Frankish A, Gilbert J, Gonzalez JM, Griffiths E, Harte R, Hendrix DA, Howald C, Hunt T, Jungreis I, Kay M, Khurana E,
748 Kokocinski F, Leng J, Lin MF, Loveland J, Lu Z, Manthravadi D, Mariotti M, Mudge J, Mukherjee G, Notredame C, Pei B, Rodriguez JM, Saunders G, Sboner A, Searle S, Sisu
750 C, Snow C, Steward C, Tanzer A, Tapanari E, Tress ML, Baren MJ van, Walters N, Washietl S, Wilming L, Zadissa A, Zhang Z, Brent M, Haussler D, Kellis M, Valencia A,
752 Gerstein M, Reymond A, Guigó R, Harrow J, Hubbard TJ, Landt SG, Frietze S, Abyzov A, Addleman N, Alexander RP, Auerbach RK, Balasubramanian S, Bettinger K,
754 Bhardwaj N, Boyle AP, Cao AR, Cayting P, Charos A, Cheng Y, Cheng C, Eastman C, Euskirchen G, Fleming JD, Grubert F, Habegger L, Hariharan M, Harmanci A, Iyengar S,
756 Jin VX, Karczewski KJ, Kasowski M, Lacroute P, Lam H, Lamarre-Vincent N, Leng J, Lian J, Lindahl-Allen M, Min R, Miotto B, Monahan H, Moqtaderi Z, Mu XJ, O'Geen H,
758 Ouyang Z, Patacsil D, Pei B, Raha D, Ramirez L, Reed B, Rozowsky J, Sboner A, Shi M, Sisu C, Slifer T, Witt H, Wu L, Xu X, Yan K-K, Yang X, Yip KY, Zhang Z, Struhl K,
760 Weissman SM, Gerstein M, Farnham PJ, Snyder M, Tenenbaum SA, Penalva LO, Doyle F, Karmakar S, Landt SG, Bhanvadia RR, Choudhury A, Domanus M, Ma L, Moran J,
762 Patacsil D, Slifer T, Victorsen A, Yang X, Snyder M, White KP, Auer T, Centanin L, Eichenlaub M, Gruhl F, Heermann S, Hoeckendorf B, Inoue D, Kellner T, Kirchmaier S,
764 Mueller C, Reinhardt R, Schertel L, Schneider S, Sinn R, Wittbrodt B, Wittbrodt J, Weng Z, Whitfield TW, Wang J, Collins PJ, Aldred SF, Trinklein ND, Partridge EC, Myers RM,
766 Dekker J, Jain G, Lajoie BR, Sanyal A, Balasundaram G, Bates DL, Byron R, Canfield TK, Diegel MJ, Dunn D, Ebersol AK, Frum T, Garg K, Gist E, Hansen RS, Boatman L,
768 Haugen E, Humbert R, Jain G, Johnson AK, Johnson EM, Kutyavin TV, Lajoie BR, Lee K, Lotakis D, Maurano MT, Neph SJ, Neri FV, Nguyen ED, Qu H, Reynolds AP, Roach
770 V, Rynes E, Sabo P, Sanchez ME, Sandstrom RS, Sanyal A, Shafer AO, Stergachis AB, Thomas S, Thurman RE, Vernot B, Vierstra J, Vong S, Wang H, Weaver MA, Yan Y,
772 Zhang M, Akey JM, Bender M, Dorschner MO, Groudine M, MacCoss MJ, Navas P, Stamatoyannopoulos G, Kaul R, Dekker J, Stamatoyannopoulos JA, Dunham I, Beal K,
774 Brazma A, Flicek P, Herrero J, Johnson N, Keefe D, Lukk M, Luscombe NM, Sobral D, Vaquerizas JM, Wilder SP, Batzoglou S, Sidow A, Hussami N, Kyriazopoulou-

776 Panagiotopoulou S, Libbrecht MW, Schaub MA, Kundaje A, Hardison RC, Miller W, Giardine B, Harris RS, Wu W, Bickel PJ, Banfai B, Boley NP, Brown JB, Huang H, Li Q,
778 Li JJ, Noble WS, Bilmes JA, Buske OJ, Hoffman MM, Sahu AD, Kharchenko PV, Park PJ, Baker D, Taylor J, Weng Z, Iyer S, Dong X, Greven M, Lin X, Wang J, Xi HS,
780 Zhuang J, Gerstein M, Alexander RP, Balasubramanian S, Cheng C, Harmanci A, Lochovsky L, Min R, Mu XJ, Rozowsky J, Yan K-K, Yip KY & Birney E (2012) An
782 integrated encyclopedia of DNA elements in the human genome. *Nature* **489**, 57–74.

44 Roose J, Molenaar M, Peterson J, Hurenkamp J, Brantjes H, Moerer P, Wetering M van
784 de, Destrée O & Clevers H (1998) The Xenopus Wnt effector XTcf-3 interacts with Groucho-related transcriptional repressors. *Nature* **395**, 608–612.

786 45 Cavallo RA, Cox RT, Moline MM, Roose J, Polevoy GA, Clevers H, Peifer M & Bejsovec A (1998) Drosophila Tcf and Groucho interact to repress Wingless signalling
788 activity. *Nature* **395**, 604–608.

46 Tseng A-S, Engel FB & Keating MT (2006) The GSK-3 Inhibitor BIO Promotes
790 Proliferation in Mammalian Cardiomyocytes. *Chem Biol* **13**, 957–963.

47 Koca Y, Collu GM & Mlodzik M (2022) Wnt-frizzled planar cell polarity signaling in the
792 regulation of cell motility. *Curr Top Dev Biol* **150**, 255–297.

48 Sheldahl LC, Slusarski DC, Pandur P, Miller JR, Kühl M & Moon RT (2003) Dishevelled
794 activates Ca2+ flux, PKC, and CamKII in vertebrate embryos. *J Cell Biol* **161**, 769–777.

49 McQuate A, Latorre-Esteves E & Barria A (2017) A Wnt/Calcium Signaling Cascade
796 Regulates Neuronal Excitability and Trafficking of NMDARs. *Cell Reports* **21**, 60–69.

50 Riquelme R, Li L, Gambrill A & Barria A (2023) ROR2 homodimerization is sufficient to
798 activate a neuronal Wnt/calcium signaling pathway. *J Biol Chem* **299**, 105350.

51 Ohkawara B & Niehrs C (2011) An ATF2-based luciferase reporter to monitor non-
800 canonical Wnt signaling in Xenopus embryos. *Developmental Dynamics* **240**, 188–194.

52 Acebron SP, Karaulanov E, Berger BS, Huang Y-L & Niehrs C (2014) Mitotic Wnt
802 signaling promotes protein stabilization and regulates cell size. *Molecular Cell* **54**, 663–674.

804 53 Piepenburg O, Vorbrüggen G & Jäckle H (2000) Drosophila Segment Borders Result from Unilateral Repression of Hedgehog Activity by Wingless Signaling. *Mol Cell* **6**,
806 203–209.

54 Jamora C, DasGupta R, Kocieniewski P & Fuchs E (2003) Links between signal
808 transduction, transcription and adhesion in epithelial bud development. *Nature* **422**, 317–322.

810 55 Conway T, Wazny J, Bromage A, Tymms M, Sooraj D, Williams ED & Beresford-Smith B (2012) Xenome—a tool for classifying reads from xenograft samples. *Bioinformatics*
812 **28**, i172–i178.

56 Dobin A, Davis CA, Schlesinger F, Drenkow J, Zaleski C, Jha S, Batut P, Chaisson M & Gingeras TR (2012) STAR: ultrafast universal RNA-seq aligner. *Bioinformatics* **29**, 15–21.

57 Li B & Dewey CN (2011) RSEM: accurate transcript quantification from RNA-Seq data with or without a reference genome. *BMC Bioinform* **12**, 323.

58 Love MI, Huber W & Anders S (2014) Moderated estimation of fold change and dispersion for RNA-seq data with DESeq2. *Genome Biol* **15**, 550.

59 Wu T, Hu E, Xu S, Chen M, Guo P, Dai Z, Feng T, Zhou L, Tang W, Zhan L, Fu X, Liu S, Bo X & Yu G (2021) clusterProfiler 4.0: A universal enrichment tool for interpreting omics data. *Innov (Camb (Mass))* **2**, 100141.

60 Machlab D, Burger L, Soneson C, Rijli FM, Schübeler D & Stadler MB (2022) monaLisa: an R/Bioconductor package for identifying regulatory motifs. *Bioinformatics* **38**, 2624–2625.

61 Fornes O, Castro-Mondragon JA, Khan A, Lee R van der, Zhang X, Richmond PA, Modi BP, Correard S, Gheorghe M, Baranašić D, Santana-Garcia W, Tan G, Chèneby J, Ballester B, Parcy F, Sandelin A, Lenhard B, Wasserman WW & Mathelier A (2020) JASPAR 2020: update of the open-access database of transcription factor binding profiles. *Nucleic Acids Res* **48**, D87–D92.

62 Kim K, Cho J, Hilzinger TS, Nunns H, Liu A, Ryba BE & Goentoro L (2017) Two-Element Transcriptional Regulation in the Canonical Wnt Pathway. *Current Biology* **27**, 2357-2364.e5.

63 Tan G & Lenhard B (2016) TFBSTools: an R/bioconductor package for transcription factor binding site analysis. *Bioinformatics* **32**, 1555–1556.

64 Li H & Durbin R (2010) Fast and accurate long-read alignment with Burrows-Wheeler transform. *Bioinform (Oxf, Engl)* **26**, 589–95.

65 Feng J, Liu T, Qin B, Zhang Y & Liu XS (2012) Identifying ChIP-seq enrichment using MACS. *Nat Protoc* **7**, 1728–1740.

66 Carroll TS, Liang Z, Salama R, Stark R & Santiago I de (2014) Impact of artifact removal on ChIP quality metrics in ChIP-seq and ChIP-exo data. *Front Genet* **5**, 75.

67 Li Q, Brown JB, Huang H & Bickel PJ (2011) Measuring reproducibility of high-throughput experiments. *Ann Appl Stat* **5**, 1752–1779.

68 Bailey TL, Bodén M, Whitington T & Machanick P (2010) The value of position-specific priors in motif discovery using MEME. *BMC Bioinform* **11**, 179–179.

69 Whitington T, Frith MC, Johnson J & Bailey TL (2011) Inferring transcription factor complexes from ChIP-seq data. *Nucleic Acids Res* **39**, e98–e98.

70 Grant CE, Bailey TL & Noble WS (2011) FIMO: scanning for occurrences of a given motif. *Bioinformatics* **27**, 1017–1018.

71 Yu J, Yusoff PAM, Woutersen DTJ, Goh P, Harmston N, Smits R, Epstein DM, Virshup DM & Madan B (2020) The Functional Landscape of Patient-Derived RNF43 Mutations Predicts Sensitivity to Wnt Inhibition. *Cancer Res* **80**, 5619–5632.

72 Liu S, Harmston N, Glaser TL, Wong Y, Zhong Z, Madan B, Virshup DM & Petretto E (2020) Wnt-regulated lncRNA discovery enhanced by in vivo identification and CRISPRi functional validation. *Genome Med* **12**, 89.

Supporting Information

Figure legends

Figure 1. Identification and classification of genes regulated by distinct branches of the Wnt signaling pathway.

A) Near-physiologic expression of β-cat4A in HPAF-II cells. WT = parental cell line. The numbers under the lanes indicate the normalized ratio of β-catenin to β-actin.

B) β-cat4A prevents the loss of *AXIN2* expression as assessed by RT-qPCR following treatment with increasing concentrations of PORCN inhibitor ETC-159.

C) Two independent β-cat4A expressing clones (#1 and #3) form colonies in soft agar despite PORCN inhibition. Representative images from three independent plates with two replicates for each condition are shown. Quantification for cl #3 is shown in Figure S1B.

D) WT and β-cat4A tumors (cl #3) were harvested for RNA-seq at four distinct timepoints following treatment with ETC-159 (37.5 mg/kg every 12 hours by oral gavage). n = 3 tumors for WT and 5 tumors for β-cat4A at each time point for a total of 32 tumors sequenced.

E) Differential expression analysis identified 3,346 genes that sorted into seven β-catenin dependent clusters and three β-catenin independent clusters of genes (see Methods). Heatmap shows log2 fold change for multiple comparisons of interest. β-cat4A vs WT at 0 h shows the differences in expression between the two conditions at 0 h. Changes in gene expression over time (compared to 0 h) are shown for tumors generated from WT HPAF-II cells (WT timecourse) and mutant β-catenin cells (β-cat4A timecourse). Also displayed are interaction terms representing the difference between these values after controlling for differences in baseline expression. DA is dependent, activated, DR is dependent, repressed, DN is dependent noise, IA in independent activated, IR is independent repressed.

F) 554 genes were identified as significantly differentially expressed at baseline (WT 0 h vs β-cat4A 0 h), distributed across each of the β-catenin dependent clusters.

Figure 2. Identification of β-catenin dependent and independent genes,

Examples of Wnt target genes identified in this analysis. For each gene, the expression (normalized counts) of the gene is shown, as are the fold changes and how these changes correspond to the heatmap representation used in Figure 1E.

A) *AXIN2* is a β-catenin dependent Wnt-activated gene, in cluster DA1.

B) *DEPTOR* is a β-catenin dependent Wnt-repressed gene (DR1).

C) *PROCA1* is a β-catenin independent Wnt-activated gene (IA1).

D) *ABCA6* is a β-catenin independent Wnt-repressed gene (IR1).

Figure 3: β-catenin independent and dependent clusters are enriched for distinct pathways, processes and TFBS motifs.

A) Enrichments for GO biological processes and KEGG pathways for each of the clusters of β-catenin dependent and independent genes (Hypergeometric test).

B) TFBS motifs enriched in the promoters of β-catenin dependent and independent genes. Enrichment is calculated as observed divided by expected (Binomial test).

C) Sequence logo of the Negative Regulatory Element (NRE) motif, modified after [34], is found in multiple clusters and significantly enriched in a cluster of β-catenin-dependent Wnt-repressed genes (DR1) – (Binomial test).

Figure 4: The Negative Regulatory Element (NRE) is capable of repressing reporter activity and is found at binding sites of TCF7L2/β-catenin

A) Enrichment of Wnt-Responsive Elements (WREs) across multiple TCF7L2/β-catenin ChIP-seq datasets. %TP/%FP represents the ratio of the percentage of peaks identified as containing a motif (%TP) versus percentage of background sequences containing a motif (%FP).

B) Enrichment of NREs across the same datasets. While HEPG2 shows strong enrichment for NREs and WREs, it only has a small number of peaks in the dataset.

C) WREs and NREs co-occur more often than predicted by chance across TCF7L2/β-catenin peaks identified in multiple cell lines. Venn diagrams show the number of WRE and NRE motifs identified and the overlap between them; significance was calculated using Fishers Exact test.

D) Addition of NREs represses, while WREs activates a minimal reporter (MimRep) in HCT116 cells driven by stabilized β-catenin. Student's t-test for panels D-E. The data are presented as mean ± standard error of the mean (SEM) of n = 6 independent biological replicates spread over 3 separate experiments.

E) The same reporters are not Wnt-regulated in HT1080 Wnt-low cells. Data are presented as mean ± SEM of n = 4 independent biological replicates from two separate experiments.

Figure 5: The Negative Regulatory Element (NRE) is necessary for the repression of the Wnt-repressed/β-catenin-dependent lncRNA ABHD11-AS1.

A) *ABHD11-AS1* is a Wnt-repressed gene in orthotopic model of HPAF-II Wnt-addicted cancer where its expression increases following PORCN inhibition. Data replotted from [7,72], n = 5-7 tumors as indicated.

B) Positions of putative Wnt-Responsive Elements (WREs) and NREs in the promoter of *ABHD11-AS1*

C) *ABHD11-AS1* expression is repressed when β-catenin signaling is activated by inhibition of GSK3 with BIO. Student's t-test for panels C-H, n = 2 independent biological replicates in one experiment.

D) Inhibiting β-catenin using CRISPR or E) siRNA leads to an increase in expression of *ABHD11-AS1* in cultured HPAF-II and HCT116 cells respectively. n = 3 independent biological replicates.

F) Expression of *ABHD11-AS1* increases in WT but not β-cat4A HPAF-II cells following Wnt inhibition with ETC-159. n = 3 independent biological replicates.

G) Transcriptional activity of *ABHD11-AS1* reporter construct in HCT116 cells following serial deletion of sequences containing WREs and NREs. n = 6 independent biological replicates. Data are representative of three independent experiments.

H) Transcriptional activity of *ABHD11-AS1* reporter construct in HCT116 cells following mutation of the two NRE sites. n = 2-6 independent biological replicates. Data are representative of three independent experiments.

Figure 6: The Negative Regulatory Element (NRE) modulates expression of the Wnt-activated/β-catenin-dependent gene *AXIN2*.

A) *AXIN2* is a Wnt-activated gene in an orthotopic model of HPAF-II Wnt-addicted cancer where its expression decreases following PORCN inhibition (data from [7], n = 5-7 independent biological replicates).

B) Positions of putative Wnt-Responsive Elements (WREs) and NREs in the promoter of *AXIN2*.

C) Transcriptional activity of *AXIN2* reporter construct in HCT116 cells following removal of the sequence containing NRE (ΔN1) leads to increased reporter expression. Student's t-test for panels C-D, n = 6 independent biological replicates. Data are representative of three independent experiments.

D) Removal or mutation of the NRE increases the transcriptional activity of the *AXIN2* promoter in HCT116 cells. n = 4-8 independent biological replicates. Data are representative of three independent experiments.

Figure 1

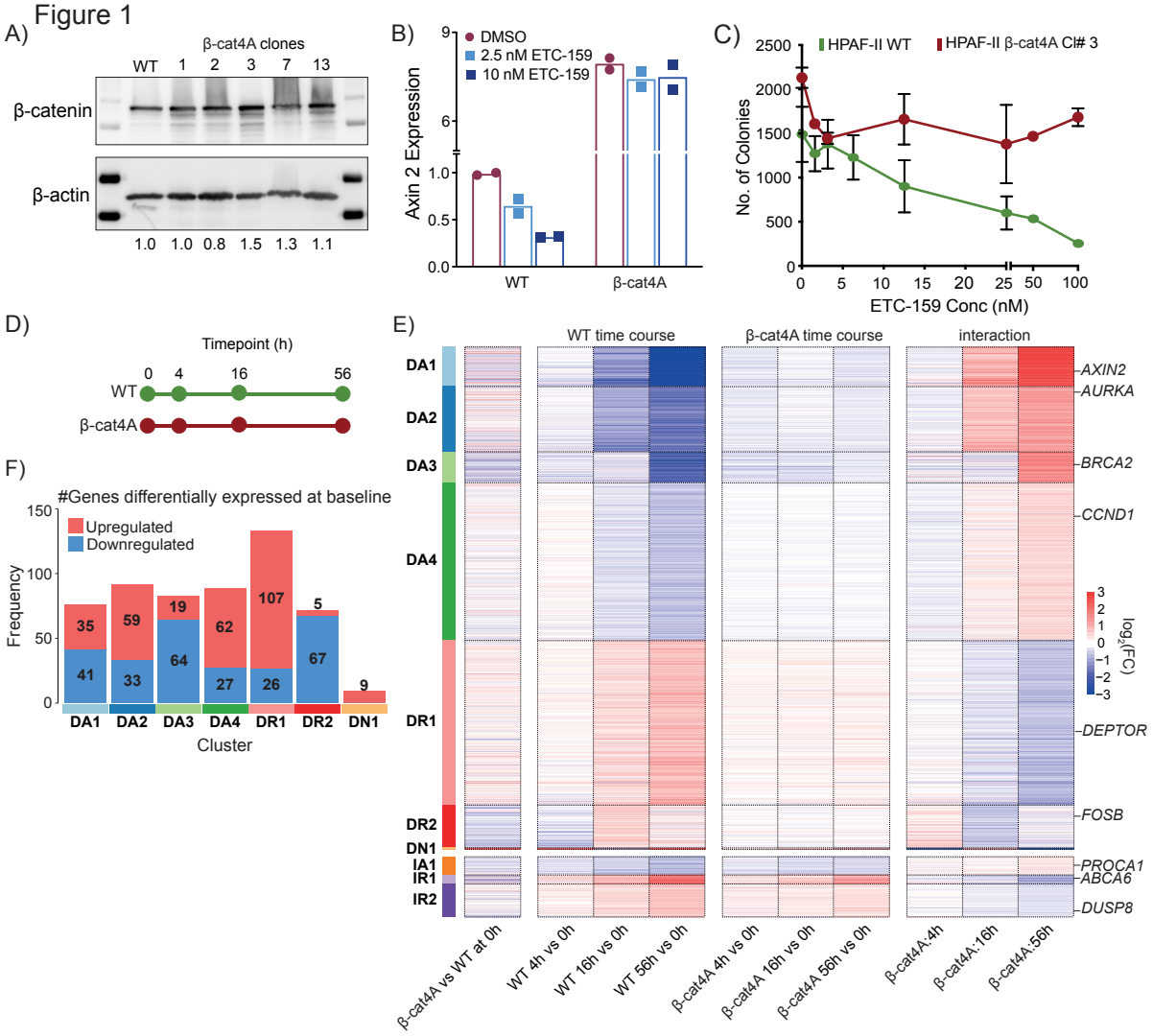
A)
β-cat4A clones
WT 1 2 3 7 13
β-catenin
β-actin
1.0 1.0 0.8 1.5 1.3 1.1
B)
DMSO
2.5 nM ETC-159
10 nM ETC-159
Axin 2 Expression
WT
β-cat4A
C)
HPAF-II WT
HPAF-II β-cat4A Cl# 3
No. of Colonies
ETC-159 Conc (nM)
D)
Timepoint (h)
0 4 16 56
WT
β-cat4A
E)
WT time course
β-cat4A time course
interaction
DA1
DA2
DA3
DA4
DR1
DR2
DN1
IA1
IR1
IR2
AXIN2
AURKA
BRCA2
CCND1
DEPTOR
FOSB
PROCA1
ABCA6
DUSP8
log2(FC)
β-cat4A vs WT at 0h
WT 4h vs 0h
WT 16h vs 0h
WT 56h vs 0h
β-cat4A 4h vs 0h
β-cat4A 16h vs 0h
β-cat4A 56h vs 0h
β-cat4A:4h
β-cat4A:16h
β-cat4A:56h
F)
#Genes differentially expressed at baseline
Upregulated
Downregulated
Frequency
35 59 19 62 107 5
41 33 64 27 26 67 9
DA1 DA2 DA3 DA4 DR1 DR2 DN1
Cluster

Figure 2

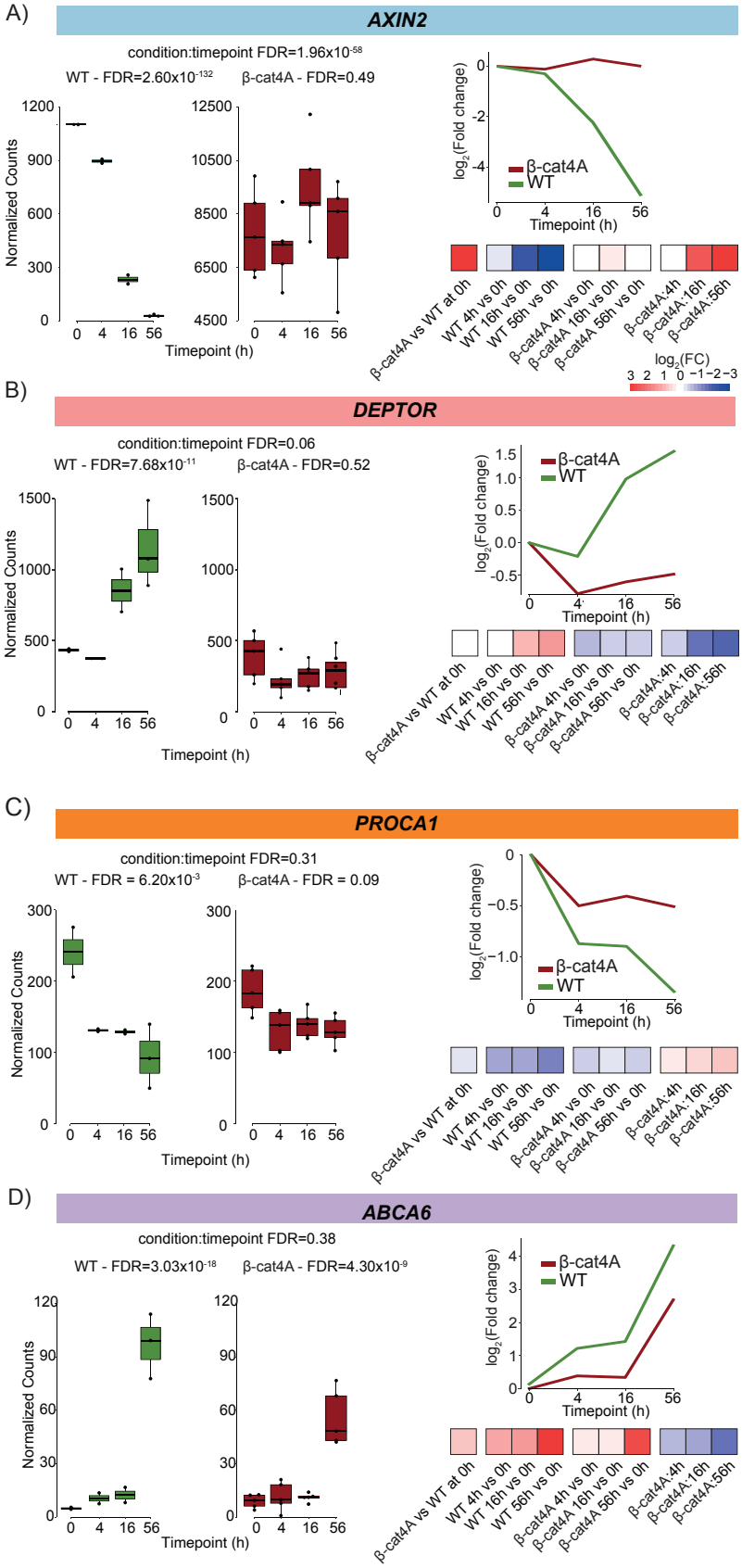
A)
AXIN2
condition:timepoint FDR=1.96x10-58
WT - FDR=2.60x10-132
β-cat4A - FDR=0.49
Normalized Counts
Timepoint (h)
log2(Fold change)
β-cat4A
WT
β-cat4A vs WT at 0h
WT 4h vs 0h
WT 16h vs 0h
WT 56h vs 0h
β-cat4A 4h vs 0h
β-cat4A 16h vs 0h
β-cat4A 56h vs 0h
β-cat4A:4h
β-cat4A:16h
β-cat4A:56h
log2(FC)
B)
DEPTOR
condition:timepoint FDR=0.06
WT - FDR=7.68x10-11
β-cat4A - FDR=0.52
C)
PROCA1
condition:timepoint FDR=0.31
WT - FDR = 6.20x10-3
β-cat4A - FDR = 0.09
D)
ABCA6
condition:timepoint FDR=0.38
WT - FDR=3.03x10-18
β-cat4A - FDR=4.30x10-9

Figure 3

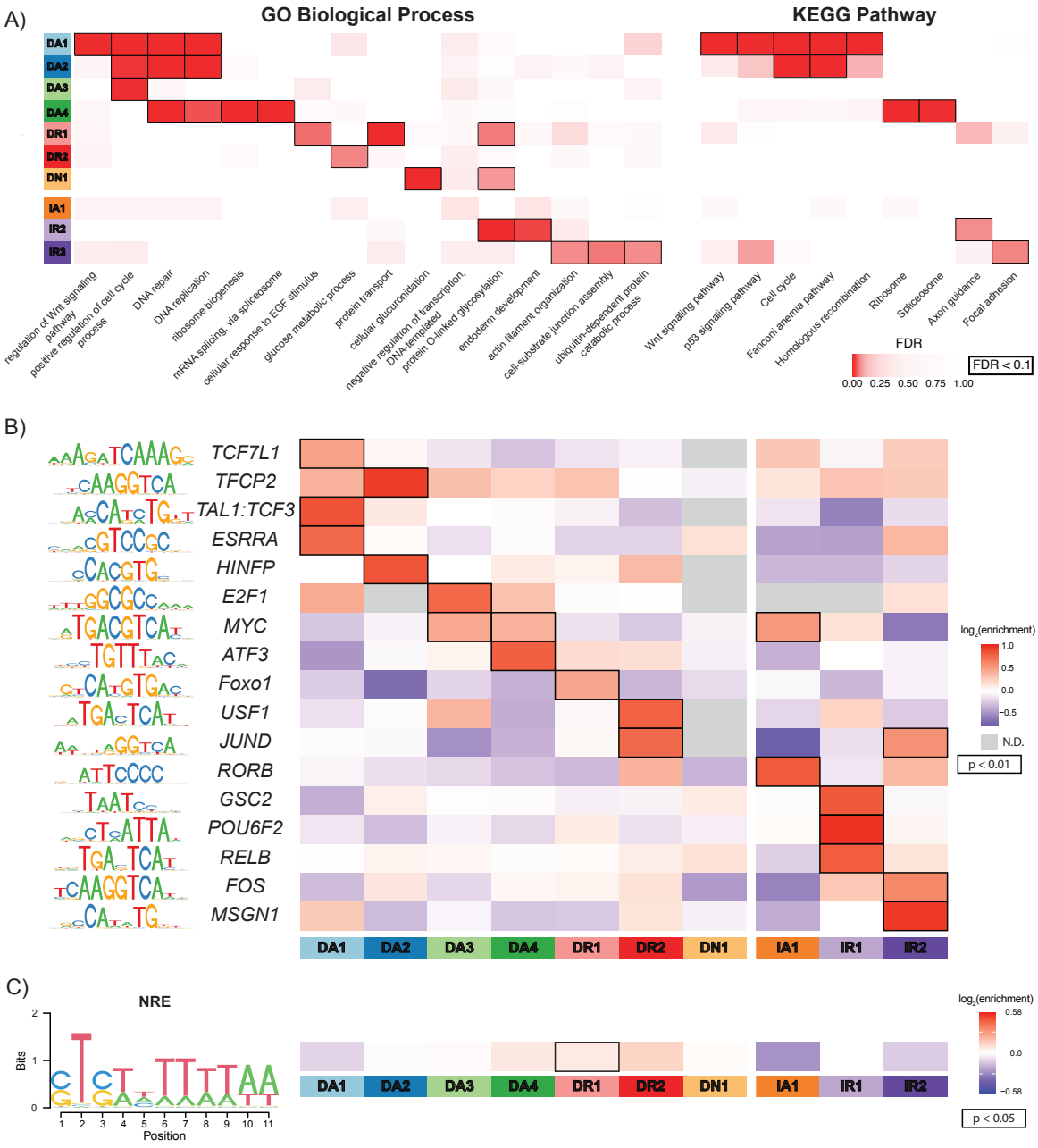
A)
GO Biological Process
KEGG Pathway
DA1
DA2
DA3
DA4
DR1
DR2
DN1
IA1
IR2
IR3
regulation of Wnt signaling pathway
positive regulation of cell cycle process
DNA repair
DNA replication
ribosome biogenesis
mRNA splicing, via spliceosome
cellular response to EGF stimulus
glucose metabolic process
protein transport
cellular glucuronidation
negative regulation of transcription, DNA-templated
protein O-linked glycosylation
endoderm development
actin filament organization
cell-substrate junction assembly
ubiquitin-dependent protein catabolic process
Wnt signaling pathway
p53 signaling pathway
Cell cycle
Fanconi anemia pathway
Homologous recombination
Ribosome
Spliceosome
Axon guidance
Focal adhesion
FDR
0.00 0.25 0.50 0.75 1.00
FDR < 0.1
B)
TCF7L1
TFCP2
TAL1:TCF3
ESRRA
HINFP
E2F1
MYC
ATF3
Foxo1
USF1
JUND
RORB
GSC2
POU6F2
RELB
FOS
MSGN1
log2(enrichment)
1.0
0.5
0.0
−0.5
N.D.
p < 0.01
DA1
DA2
DA3
DA4
DR1
DR2
DN1
IA1
IR1
IR2
C)
NRE
Bits
Position
log2(enrichment)
0.58
0.0
−0.58
p < 0.05

Figure 4

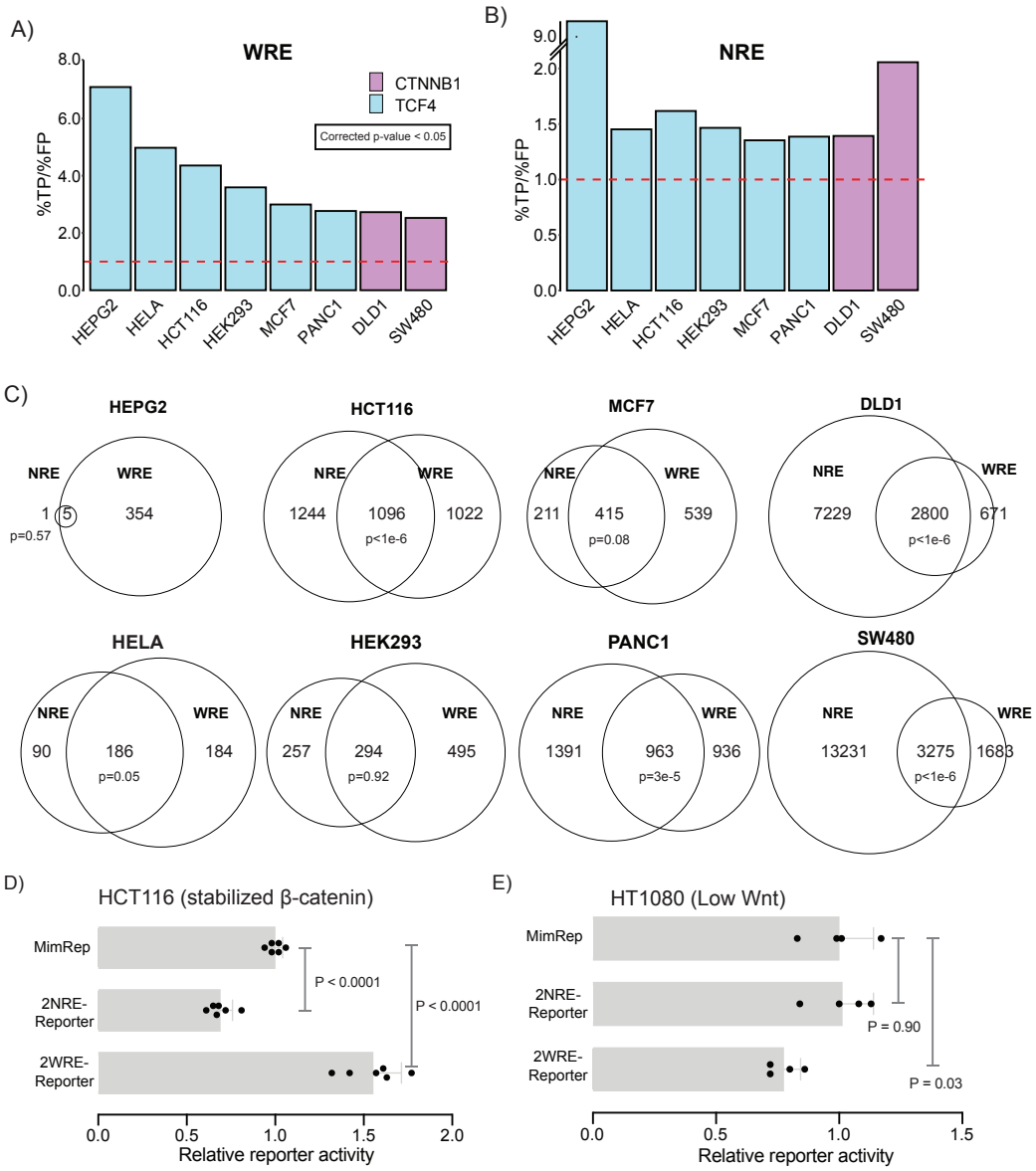
A)
WRE
CTNNB1
TCF4
Corrected p-value < 0.05
%TP/%FP
HEPG2
HELA
HCT116
HEK293
MCF7
PANC1
DLD1
SW480
B)
NRE
C)
HEPG2
NRE
WRE
1
5
354
p=0.57
HCT116
1244
1096
1022
p<1e-6
MCF7
211
415
539
p=0.08
DLD1
7229
2800
671
p<1e-6
HELA
90
186
184
p=0.05
HEK293
257
294
495
p=0.92
PANC1
1391
963
936
p=3e-5
SW480
13231
3275
1683
p<1e-6
D)
HCT116 (stabilized β-catenin)
MimRep
2NRE-Reporter
2WRE-Reporter
P < 0.0001
P < 0.0001
Relative reporter activity
E)
HT1080 (Low Wnt)
P = 0.90
P = 0.03
Relative reporter activity

Figure 5

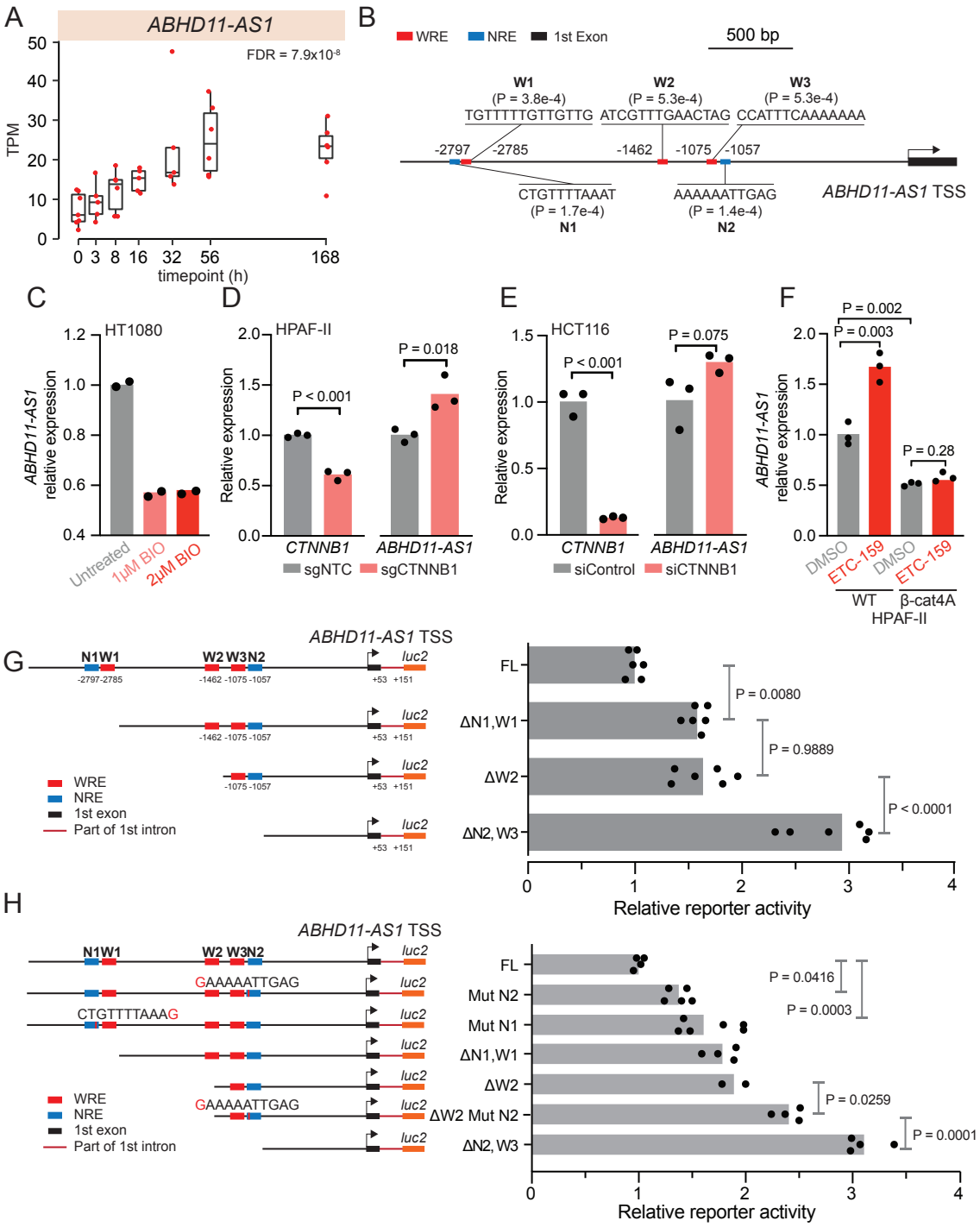
A
ABHD11-AS1
FDR = 7.9x10-8
TPM
timepoint (h)
B
WRE
NRE
1st Exon
500 bp
W1
(P = 3.8e-4)
TGTTTTTGTTGTTG
W2
(P = 5.3e-4)
ATCGTTTGAACTAG
W3
(P = 5.3e-4)
CCATTTCAAAAAAA
-2797
-2785
-1462
-1075
-1057
CTGTTTTAAAT
(P = 1.7e-4)
N1
AAAAAATTGAG
(P = 1.4e-4)
N2
ABHD11-AS1 TSS
C
HT1080
ABHD11-AS1 relative expression
Untreated
1μM BIO
2μM BIO
D
HPAF-II
Relative expression
P < 0.001
P = 0.018
CTNNB1
ABHD11-AS1
sgNTC
sgCTNNB1
E
HCT116
P < 0.001
P = 0.075
siControl
siCTNNB1
F
P = 0.002
P = 0.003
P = 0.28
DMSO
ETC-159
WT
β-cat4A
HPAF-II
G
ABHD11-AS1 TSS
N1W1
W2 W3N2
luc2
WRE
NRE
1st exon
Part of 1st intron
FL
ΔN1,W1
ΔW2
ΔN2, W3
P = 0.0080
P = 0.9889
P < 0.0001
Relative reporter activity
H
ABHD11-AS1 TSS
GAAAAATTGAG
CTGTTTTAAAG
Mut N2
Mut N1
ΔW2 Mut N2
P = 0.0416
P = 0.0003
P = 0.0259
P = 0.0001
Relative reporter activity

Figure 6

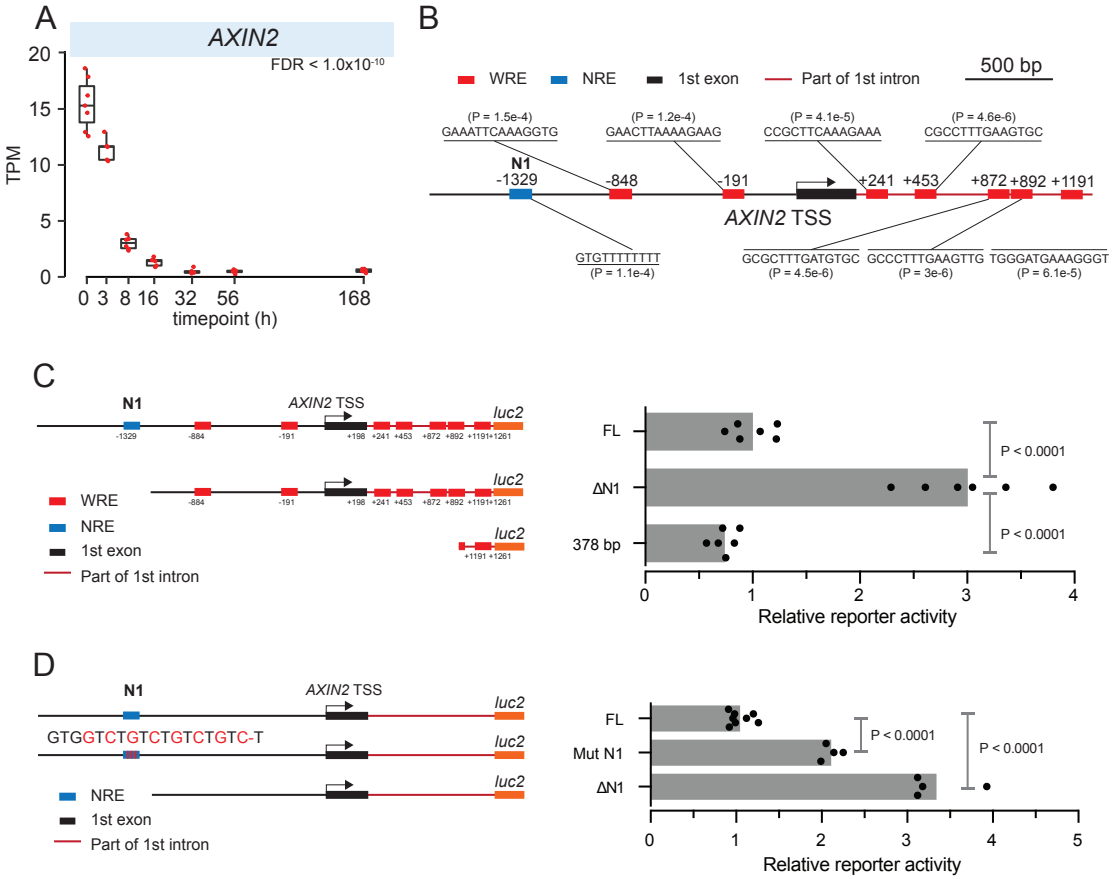

1008

1010

Supplemental Figure 1

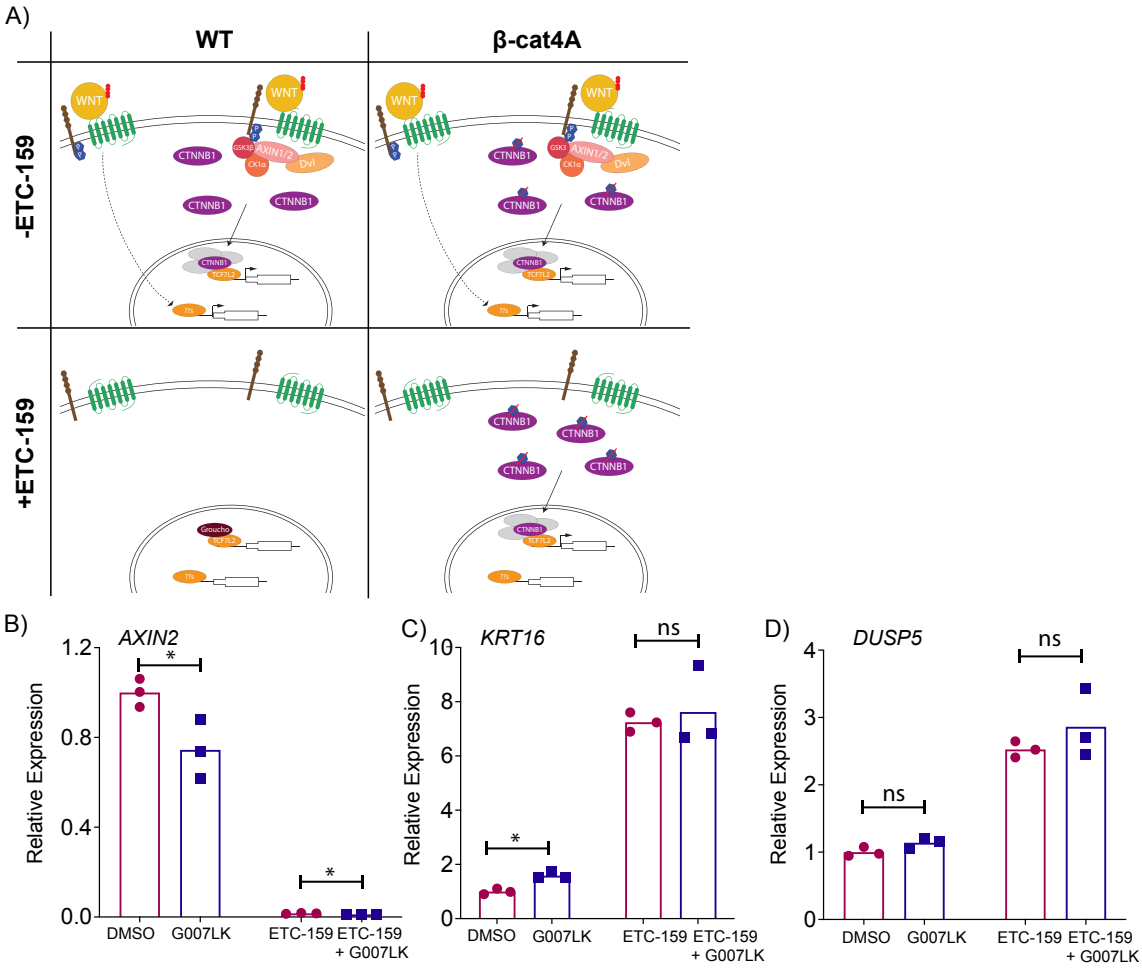

Supplemental Figure 2

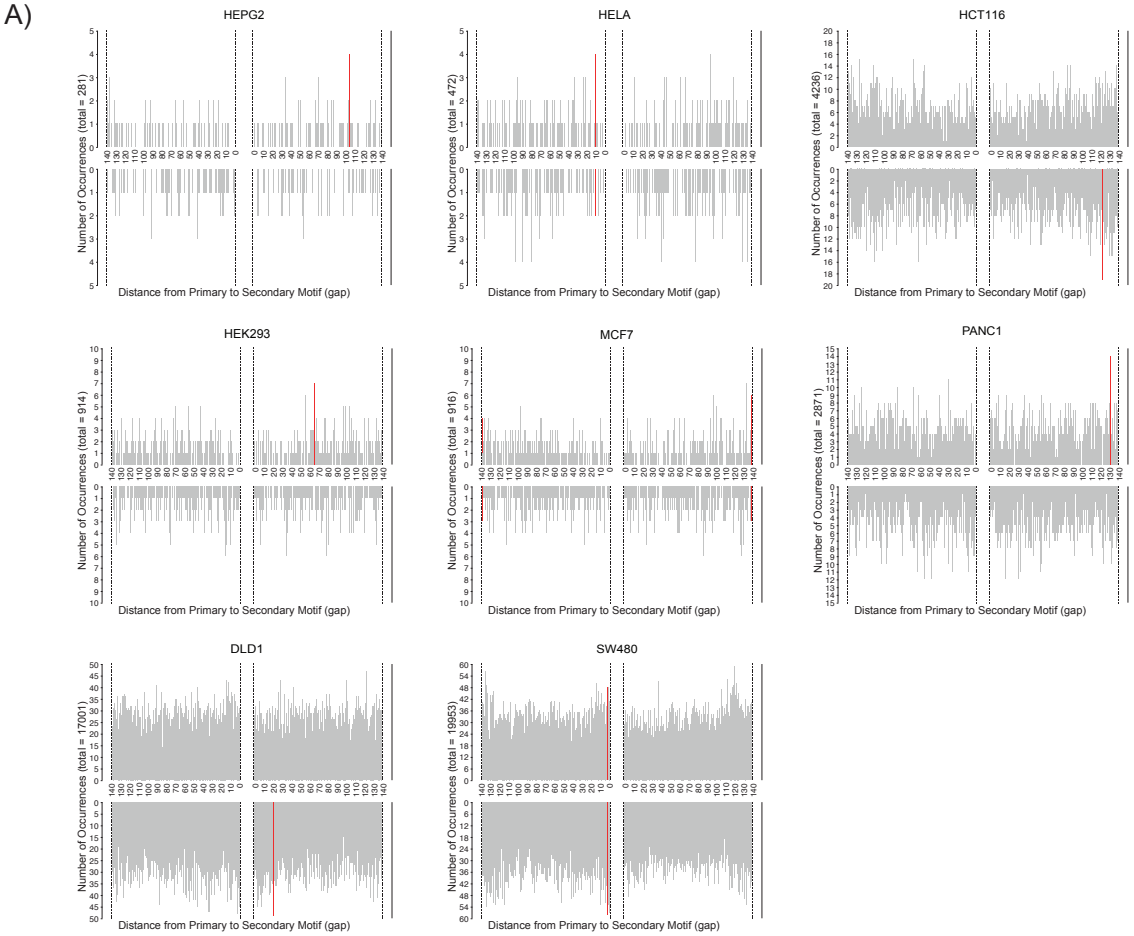

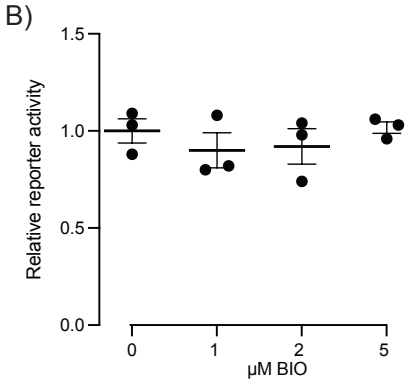

Supplemental Figure 3

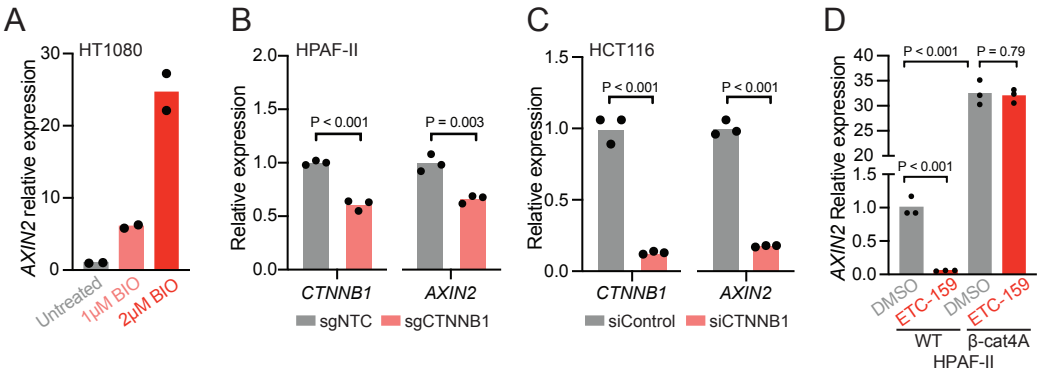

1026

1028